ARC Linkage Project Report (LP0560270)

Research Report No: 2006/16

Review of Contact and Dynamic Phenomena in Cold Roll Forming

Alexander S. Galakhar, William J.T. Daniel
and Paul A. Meehan

Division of Mechanical Engineering
School of Engineering

The University of Queensland

August 2006

Contents

1. Historical outline

The Second Industrial Revolution resulted in a rapid economic growth and emergence of thriving automobile industry. A strong demand for cars determined the increasing requirement for light thin walled steel structures and had a strong technological impact on sheet metal forming. The conventional stamping technology required large and expensive stamping presses for making long thin-walled parts. The size of the thin-walled parts was limited with the press equipment approximately at 1 m, the equipment had long idle running and the stamping process required auxiliary manufacturing operations [106]. The requirement of a reduction of both production time and cost of long thin-walled parts lead to the creation of the cold roll forming (CRF) process [106].

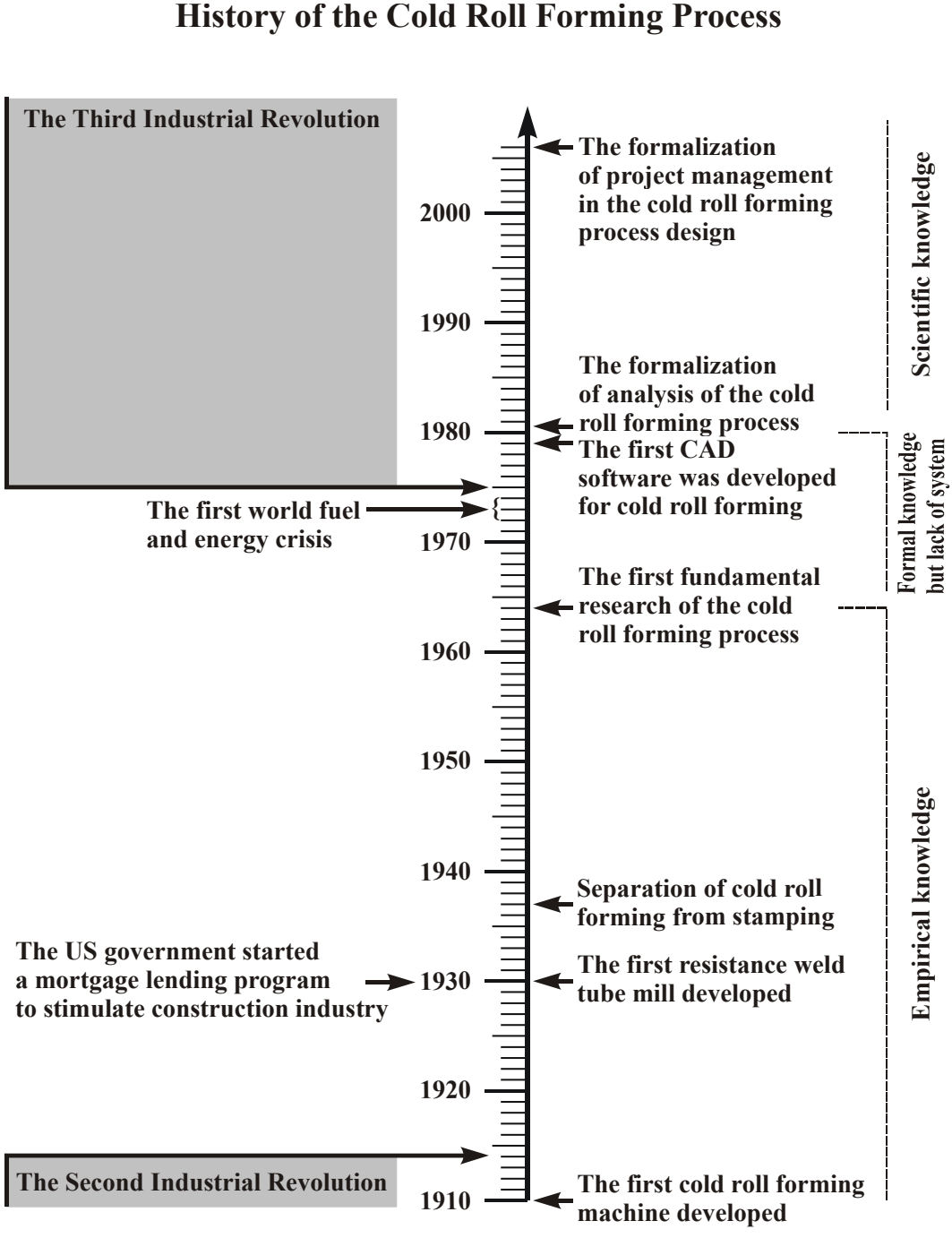

Fig. 1. *History of the CRF process*

The world first continuous CRF machine was developed by Carl M. Yoder in 1910 in the USA (fig. 1). It was the Yoder Y-70 Mud Strip Forming Machine for the production of automobile mud strips.

CRF technology provided large technological advantages in thin-walled parts manufacturing compared to press forming, as it did not require too many auxiliary operations, the CRF equipment had no idle running and the length of the parts was not limited with the equipment any more [106]. The last fact made the light thin-walled structures obtained with the CRF process especially attractive to the construction industry [106]. Yoder's company developed the first commercially available resistance weld tube mill in 1930. It was the first continuous weld pipe mill that could produce 660 mm tubes.

The CRF process was only considered as a type of stamping process until 1937 and the abundant experience gained in stamping was applied to the new equipment that time. But due to contact and dynamic phenomena taking place during the CRF process and the distinct technological operations made it necessary to distinguish CRF from stamping and rolling [106].

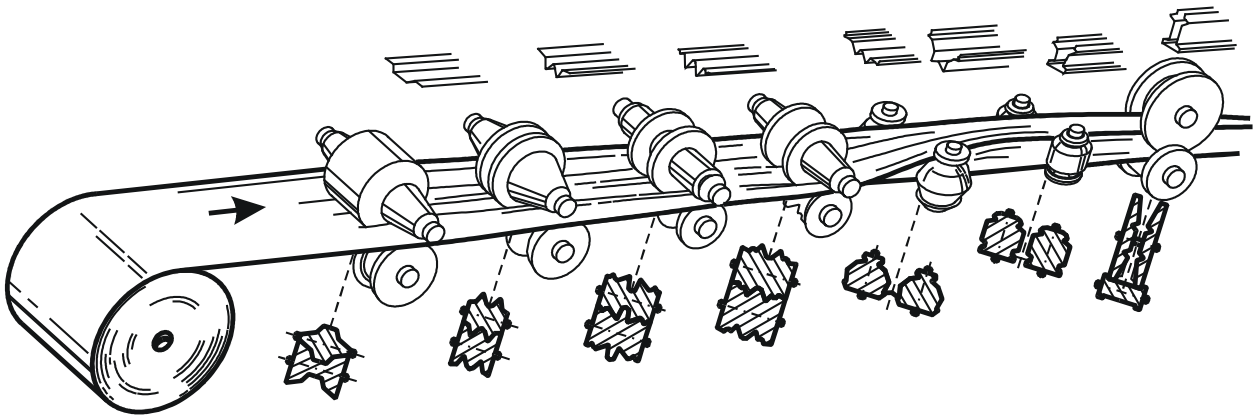

Fig. 2. *A typical CRF process* [32]

Roll forming was defined as a process whereby "a flat strip of metal is progressively formed into a desired cross-section by passing through a series of rolls arranged in tandem" [106] (fig. 2). It is increasingly used in modern sheet-metal industry because the process satisfies the modern requirements of high productivity, environmental quality, quality maintenance, high accuracy and uniformity of parts, consistency of properties and surface conditions [2]. Painted and electroplated materials can also be formed without damage to the coating [2]. Although the primary function of CRF is to make a desired shape of flat strip, the versatility of this method has also been extended through incorporation of other operations into the process. The operations usually combined with CRF are automatic cutting off, piercing, crimping, marking, bulging, curving and coiling.

Until the 1970s, the design of both the tools geometry and the CRF mill had relied on empirical formulae based on the experience of the roll designers and the roll setters [1, 92-96]. The use of empirical formulae was promoted by the lack of formal experimental and theoretical studies of CRF and partly by the inability to perform the sophisticated computations in plant conditions quickly at that time. At this time the rapid development of and growing demand for diverse new cold roll formed products of higher quality made it very difficult to control the process through the use of empirical knowledge and attracted more researchers to study CRF in a more fundamental manner [7, 38, 57, 58, 62, 81, 105].

The industry needed a more formal scientific approach to the CRF process analysis in the theatre of rugged competition in the 1970s. This stimulated experimental study focused on the creation of more complex mathematical models of the CRF process intended for use with quickly developing computer technology [40, 42, 47]. The use of computers allowed numerical analysis to take into account the influence of the contact conditions on the CRF process. The first attempt to obtain experimental evaluation of contact pressure in the CRF process was made by Kato [38] in 1963. The first extensive experimental study of contact pressure in the CRF process was made by Suzuki et al in 1976 [85] and followed up by Kiuchi in 1979 [43]. The first scientific study of the effects of buckling

and strip distortion was performed by Suzuki et al in 1977 [86]. This and subsequent research revealed the relationship between buckling of the deformed strip and the rolls geometry. That knowledge affords formulation of CRF mill design requirements. The residual stresses remaining after the CRF process, and their influence on buckling of welded cold roll formed box columns were analysed later by Ingvarsson in 1975 and 1979 [34, 35].

1974 is usually marked as the start of the Third Industrial Revolution inseparably linked with the rapid development of computer technology. The investments in IT started increasing rapidly everywhere after 1974 [25]. The first report of CAD application to CRF appeared in 1979 [75]. The revolution's two interrelated trends are the development of flexible manufacturing systems and CAD/CAE/CAM technologies that facilitate efficient design development and manufacturing application. These two trends were manifested in CRF in the 1980s. They appear in CRF technology in three forms.

1. The tool geometry became more independent of the strip profile geometry as in the vertical CRF process invented by Nakajima et al [63] that requires more sophisticated computer-oriented analysis for the engineering set-up.
2. New CAD/CAE software for the CRF process is developed rapidly and applied to production to accelerate CRF mills repurposing and to eliminate possible product defects. The CAD/CAE software incorporates the results of new scientific research, expressed in more sophisticated mathematical models of the CRF process. It was developed to reduce the number and cost of engineering set-up trials.
3. The theory concerning analysis of the CRF process tends to be more computer-oriented than empirical and the latest scientific results become incorporated into software.

The procedure of the CRF process analysis has been formalized generally both from a technical point of view in 1980 by Kiuchi [45, 46] and from an organizational point of view in 2006 by Mynors et al [61].

2. Known CRF products defects and their origins

Flaws such as surface damage and shape defects could be observed in the CRF process due to peculiarities in the tool geometry and mill settings giving rise to inadmissible contact or residual stresses in the formed strip. A detailed list of CRF product defects and general practical recommendations on their avoidance are provided by Halmos [26]. The defects affecting the surface due to undesirable contact conditions are considered as a surface damage. The shape defects are caused by residual stresses. Both types of defects should be considered when establishing optimal roll pass schedules [37].

Both shape and surface defects are discussed in the following sections.

2.1. Surface defects

The earliest empirical data on surface defects were summarized by Vanderploeg [92] and Kato [38]. They showed that the formed profile surface scoring is caused by the shoulders of the rolls (see fig. 3). The scoring could be avoided in the following ways:

1) the rolls shoulders have to be rounded with a sufficiently large radius;
2) the workpiece width has to be properly sized.

The rounded shoulders make the workpiece sliding into the groove easier. The rounding radius is limited only by the cross section design. Strip width sizing is easy if the bend angle does not exceed 90 . For 90 bending the strip is bent at first close to 90 and then its sides are bent to 90 angle with side rolls or idlers.

The first complex research devoted to CRF product defects and their origins was carried out by Jimma and Ona [37].

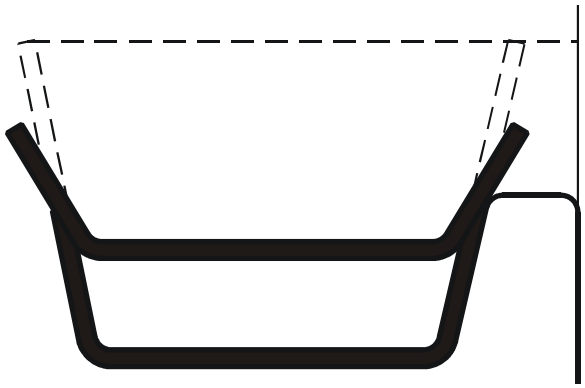

Fig. 3. Scoring the surface by the roll shoulders during CRF [92].

Jimma and Ona performed the experiments with the 42 combinations of the forming rolls depicted in fig. 4. They distinguished and investigated the following four types of surface damages [37]:

X1. Deep and narrow scoring near the flange edge indicates that forming with 85° roll is excessively severe (fig. 4).
X2. Shallow and long scoring in the middle part of the flange appears when forming with the ordinary 90° roll. The defect could not usually be eliminated completely and has to be avoided with the use of an inverse 90 roll (fig. 4).
X3. Fine identation marks from the middle to the bend of the flanges originate at the early or middle passes within the CRF process and are most conspicuous on polished surfaces of bright steel, stainless steel and aluminium which lose their splendour and become whitish (fig. 4).
X4. Narrow scoring close to the flange edge appears when forming with the inverse 90 roll. This damage is usually ignored (fig. 4).

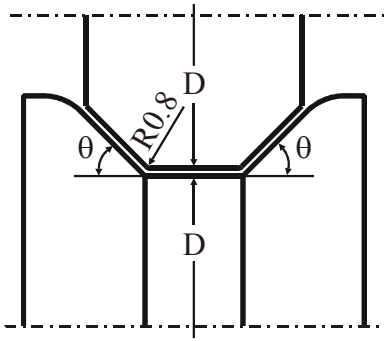

Dimensions of forming rolls

θ (degree)	D (mm)
15	135
30	135.5
45	136
60	136.5
75	137
85	137.5
90	138

Two kinds of 90° rolls

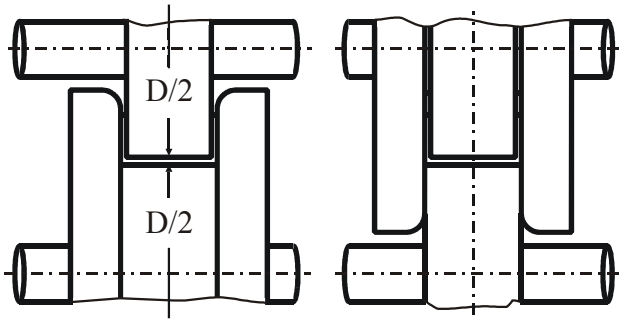

(a) ordinary rolls (b) inverse rolls

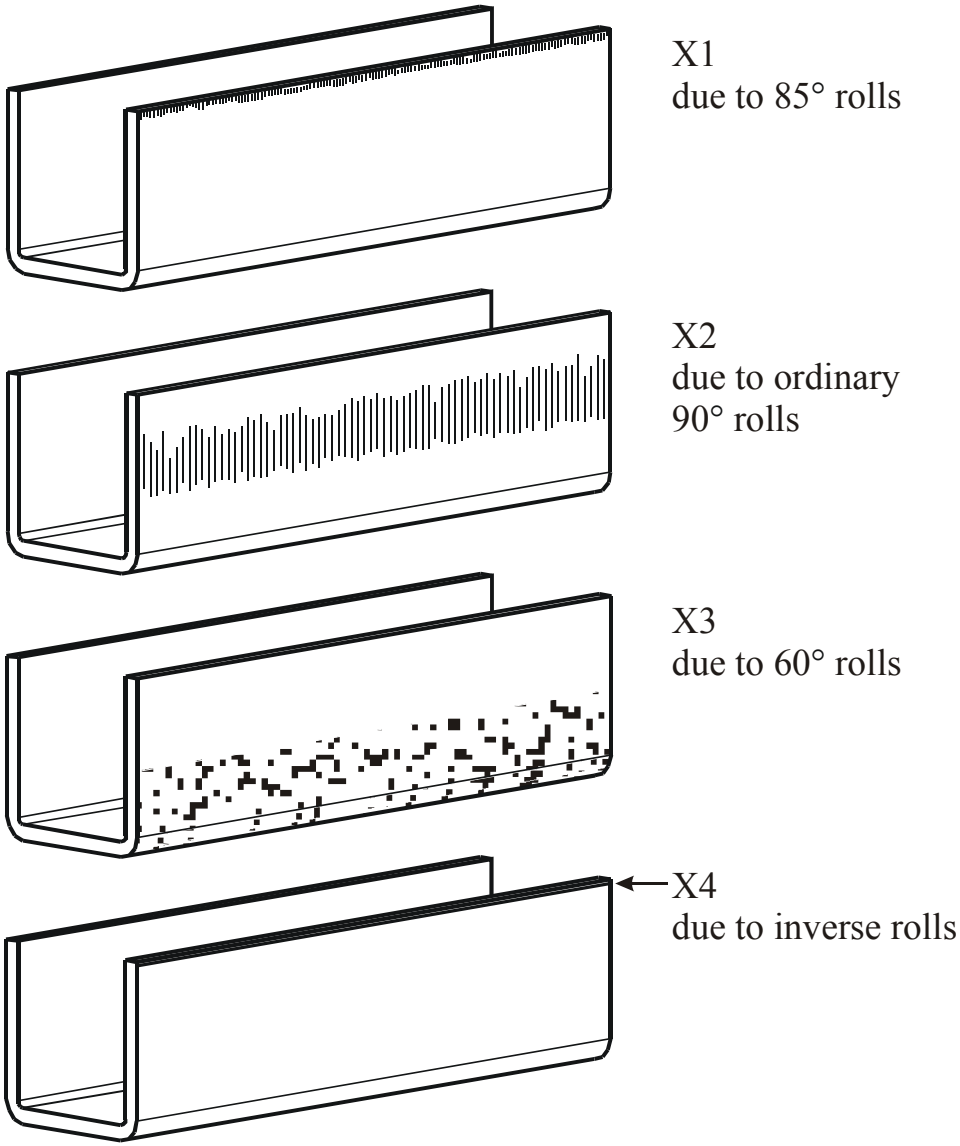

Fig. 4. Forming rolls and surface damages [37]

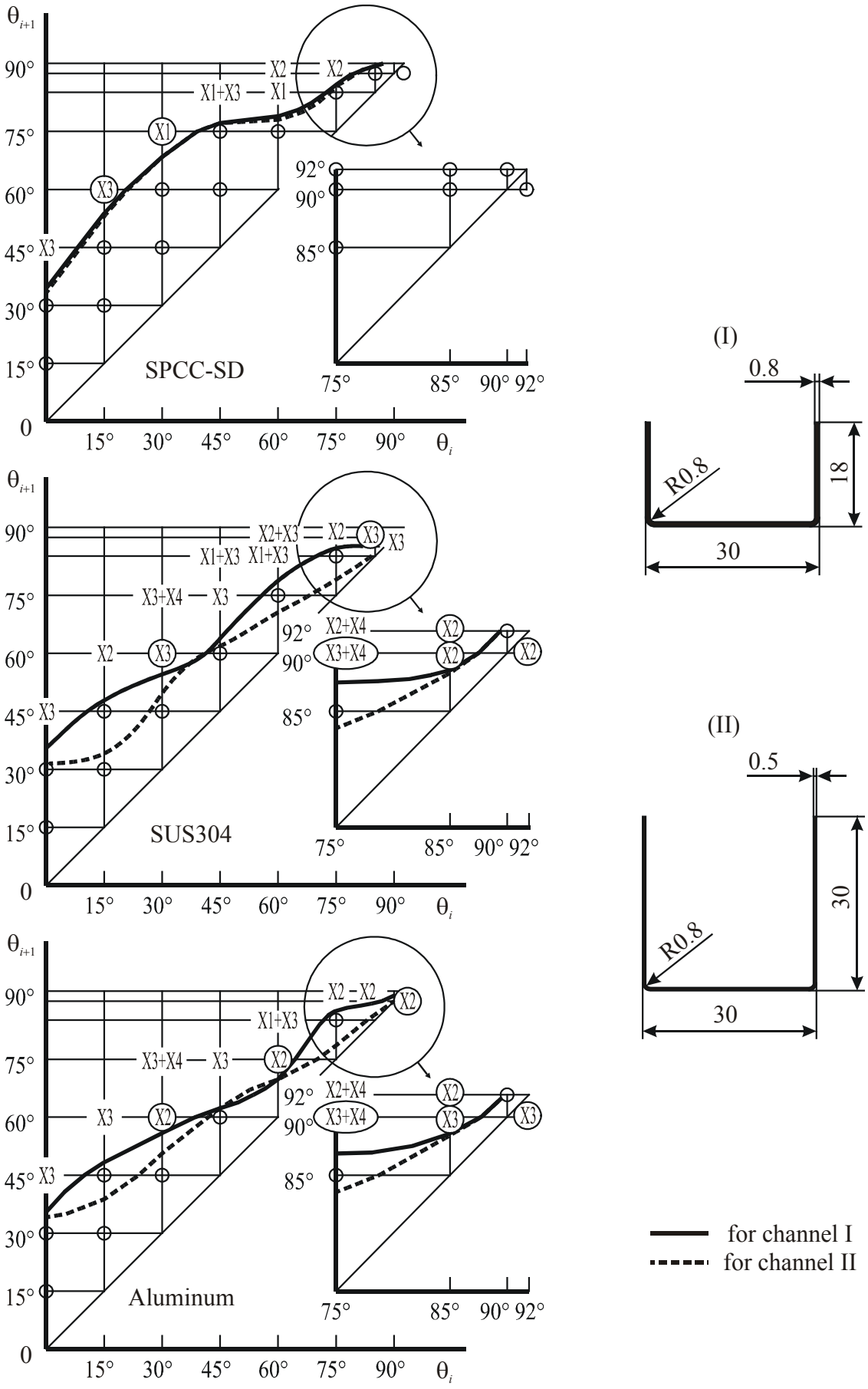

Fig. 5. Roll angles selection for producing channel profiles with minimum surface damage [37].

Jimma and Ona [37] drew three charts showing the limit of surface damage occurrence for 3 different materials (fig. 5). The solid and dotted lines correspond to channel I and channel II respectively. The presented charts show that the minimal strip surface damage takes place for the consecutive bend angles θ_i and θ_{i+1} lying under the solid or dotted curves. The surface damage types are marked with a letter X enclosed in a circle or an oval. However, the practical use of these results is limited because the authors considered a limited combination of rolls depending on the strip material and size.

2.2. Shape defects

The known shape defects occurring in CRF are shown in fig. 6. These defects are caused by strip instability through a complex distribution of residual stresses in the formed profile.

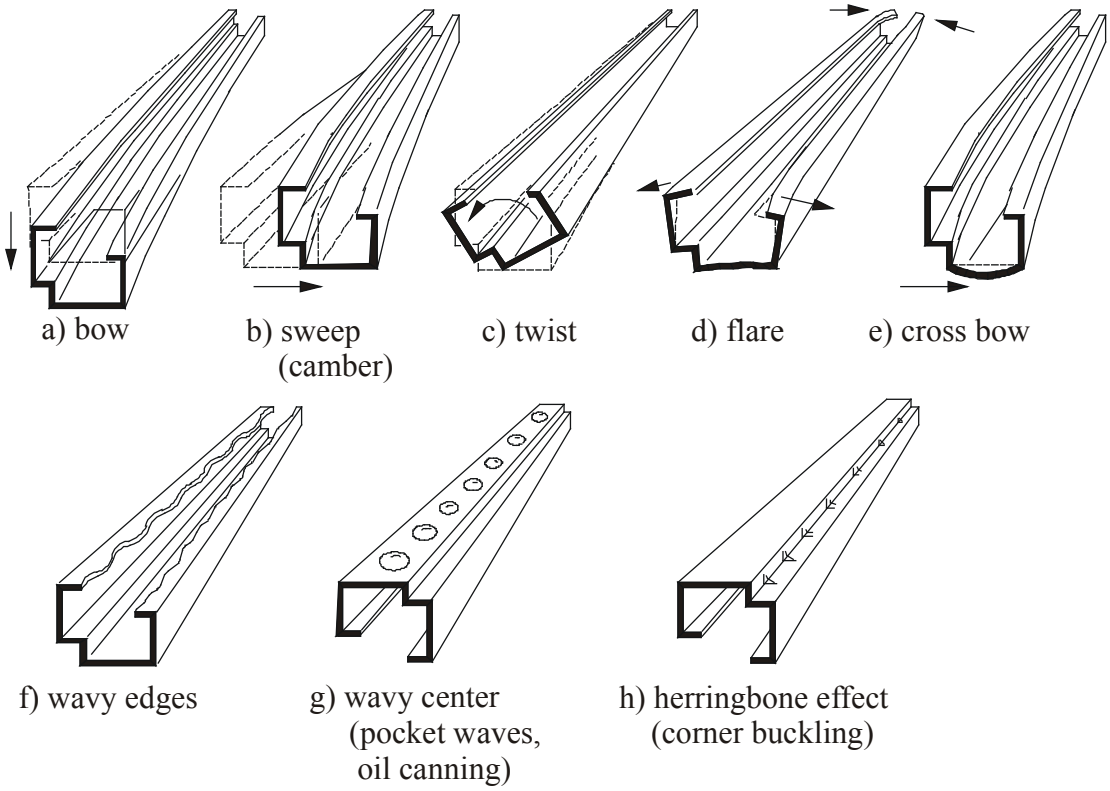

Fig. 6. Shape defects of cold roll formed profile [2]

The appearance of shape defects may be caused by the equipment, material or poor process design [26].

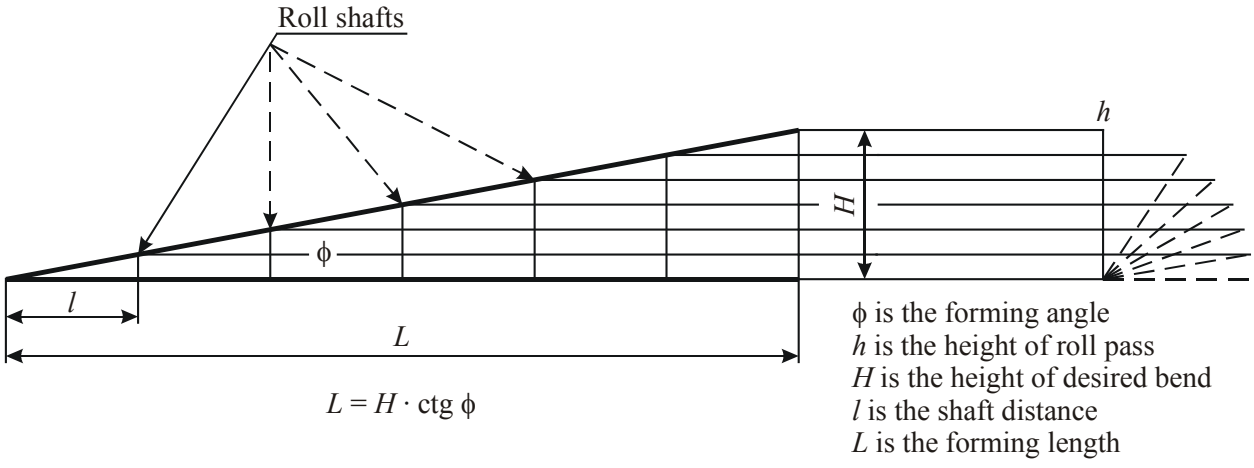

Fig. 7. Forming angle method [41].

Abundant research has been performed since 1949 to achieve a numerical prediction of these defects. Early research of shape defects was aimed only at avoiding [6] or reducing [103] the shape deviations.

Angel [6] proposed avoiding the shape defects by setting a constant forming angle (fig. 7) equal to 1.25 . However, bending in the first pass differs from bending in the last pass. Lejchenko [50] and later Sachs [78] proposed to limit the forming increment between 2 passes.

Schulze [79] obtained an expression for the edge point path between two roll stands assuming it to be a straight line, as the shortest possible distance between the stands. A similar equation was also used for edge strain estimation [19]. However the dependence of strip instability on edge strain was not investigated [19, 79].

The strip instability analyses based on empirical expressions are more efficient at present time, however theoretical research has been focused on a more formal scientific foundation.

2.2.1. Bow, camber and twist

Kato [38] and then Suzuki et al [84] noted that bow and camber (longitudinal curvatures of the formed profile along y and x axes respectively, see fig. 6) of a formed profile depend on the difference between the residual strains at the edges and centre of the formed strip cross section.

Suzuki et al [84] carried out extensive studies of the CRF process on a CRF machine with 5 roll stands for circular arc profile (strip thicknesses from 0.6 mm to 3.0 mm, strip widths from 10 mm to 180 mm), V-type profile (strip thicknesses from 0.6 mm to 3.2 mm, strip widths from 40 mm to 94 mm), trapezoidal profile (strip thicknesses from 0.6 mm to 3.0 mm, strip widths from 70 mm to 140 mm). They varied the roll clearance from 0.4 mm to 3.4 mm and revealed that the longitudinal curvature does not depend on the roll clearance for the circular profile but such dependence is obvious for V-type and trapezoidal sections when the transversal bending angle of the rolls in the stand exceeds 120°. They also investigated the influence of roll diameter on the longitudinal curvature of formed arc profiles. They found that the concave (female) roll diameter enlarging reduces the longitudinal curvature for comparatively large absolute values α_i of apparent inlet angle of sheet metal, but when α_i is close to zero the effect of roll diameter on longitudinal curvature cannot be recognized [84]. The effect of maximum diameter of convex forming roll and minimum diameter of concave roll is generally very small for trapezoidal profile and insignificant in forming V-type profile except when α_i is large enough. It seems that when the designed diameter of pitch circle divides the depth of the roll grooves into equal halves the longitudinal curvature is minimal for both profile types [84].

Kokado and Onoda [47] studied the influence of strip thickness t and width on the longitudinal curvature in CRF of top-hat profiles with a circular groove. They found that the longitudinal curvature is proportional to $t^{2.1}$ and also depends on the ratio of strip width to profile length. They found that longitudinal curvature also depends on α_i [47].

The experiments by Suzuki et al [84] and Looi [52] on V-type and trapezoidal profiles showed the influence of strip thickness t and width on the longitudinal curvature similar to Kokado and Onoda's results [47].

Kato et al [39] carried out the experiments on different materials and demonstrated that longitudinal curvature of formed inverted circular sections can be eliminated with a guide block set at a fixed height below the forming rolls pass line.

Jimma and Ona [37] studied the CRF process for symmetrical channels formed using forty-two roll pass schedules and demonstrated that the longitudinal curvature does not depend on the number of roll passes but only on the severity of forming at the last roll pass (see fig. 8). So, the curvature for the 19th schedule (45° → 75° → 85°→ 90°) is smaller than for the 36th schedule (15° → 30° → 45° → 60° → 75°→ 90°). The forming angle method being a serious simplification does not imply this result.

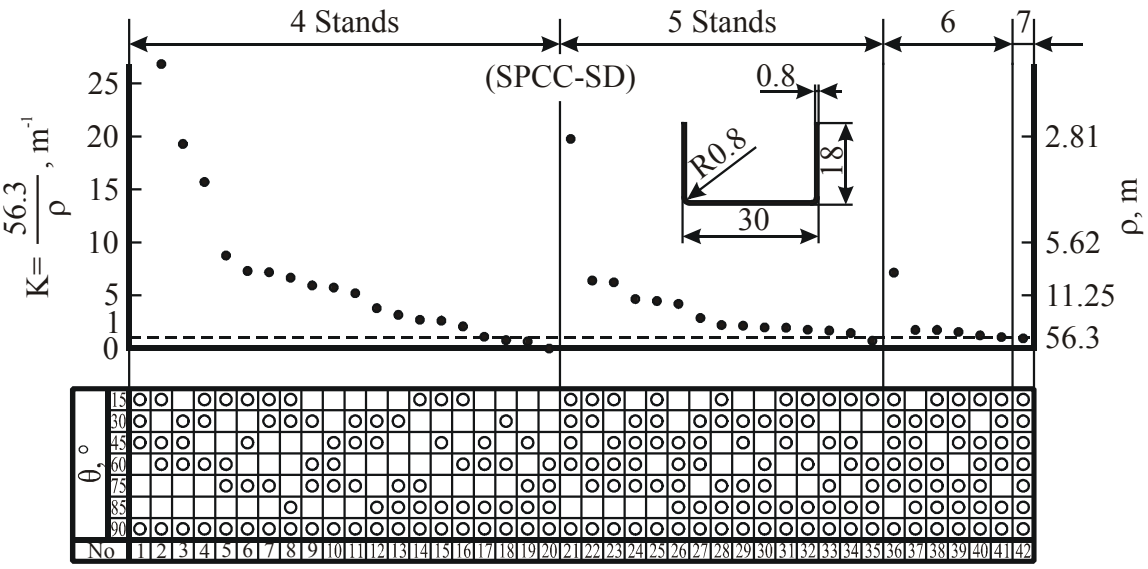

Fig. 8. Longitudinal curvature and ratio of curvatures of the formed channel section [37].

Ona et al [69] examined experimentally the longitudinal curvature and twist correction methods and found that:

1) mild distortion may be corrected with an exit straightener;
2) both twist and sweep could be effectively corrected with a transverse shift of the upper and lower rolls at the final stand, however:
   — the twist is reduced by shifting the rolls towards the lower flange side, but the sweep decreases by shifting the rolls in opposite direction;
   — the transverse shift of the rolls before the exit straightener could lead to edge buckling in the higher flange that diminishes its efficacy;
3) bow could be effectively reduced with an increase in the roll pressure at the final roll stand, but this does not affect twist and sweep;
4) both twist and bow could be eliminated with:
   — over-bend rolls set just in front of the final roll stand;
   — a combination of roll-pressure adjustment and exit straightener found to be more effective;
5) the effective twist correction could be obtained with a twist-forming stand:
   — in the position of the final roll stand;
   — ahead of the final roll stand if the roll-pressure adjustment and transverse shift of the rolls are used at the same time;
6) the over-bend rolls are most effective being added in the position following a twist-forming stand before a final roll stand, that could eliminate both twist and longitudinal curvature;
7) the shape distortions of the utterly asymmetrical channel could not be corrected with the investigated methods.

A simple formula for prediction of twist and sweep of pre-notched channel profiles was proposed by Watari and Ona [101].

Ona et al showed effective bow reduction with a back tension in their experiment [72].

2.2.2. Flare and cross bow

Such profile deformations as flare and cross bow can appear in the final cut product due to so called spring-back deformation [38, 39].

Spring-back is caused by the residual stress distribution in the final profile and can be reduced with:

1) “over-bending method” [4] when the strip is bent excessively to compensate for the spring-back deformation (see fig. 9 (a));

2) “inside-roll method” when the residual stresses induced by the forming rolls which deform the profile from outside into inside are reduced by small rolls which bend the side walls from inside to outside (see fig. 9 (b)).

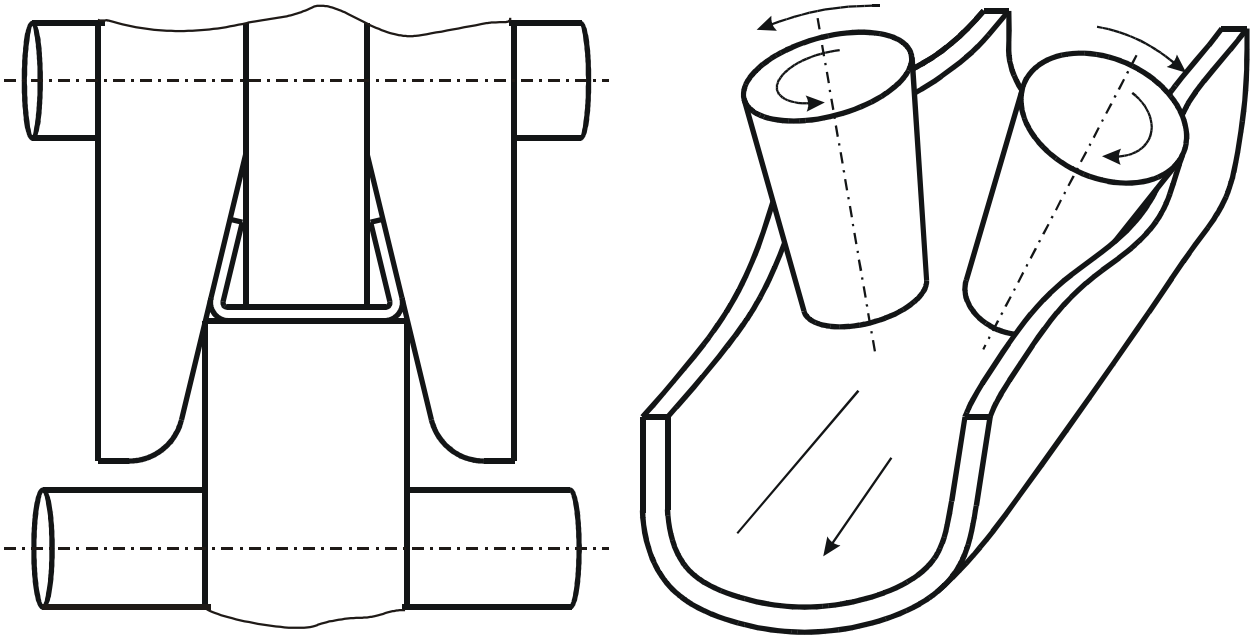

(a) over-bending method [37] (b) inside-roll method [44]

Fig. 9. Spring-back reduction.

The “over-bending method” is based on empirical fit of deformation to produce the residual stresses distribution eliminating the flare and cross bow effects in the formed profile.

The “inside-roll method” avoids the flare and the cross bow by an effective reduction of the residual stresses causing these defects.

2.2.3. Edge waves

Baba [7] investigated the edge stretch phenomenon, which causes edge waves in the manufacturing of electric resistance welded (ERW) steel tubes. He showed that the increase of the formed pipe diameter results in the increase of edge stretch, whereas the increase of female roll diameter or the increase of the roll stands number decreases the edge stretch.

Russel and Kuhn [77] noted that the length difference between the paths of edge and centre points of the profile must not exceed the elastic limit deformation known for the used material to prevent wavy edges formation, but they carried out no research of this issue.

According to the experiments [103] the edge instability could be eliminated with:

— accurate roll design guaranteeing the absence of plastic deformation in the edge;
— longitudinal tension by the driving rolls of increasing diameters;
— straightening the profile.

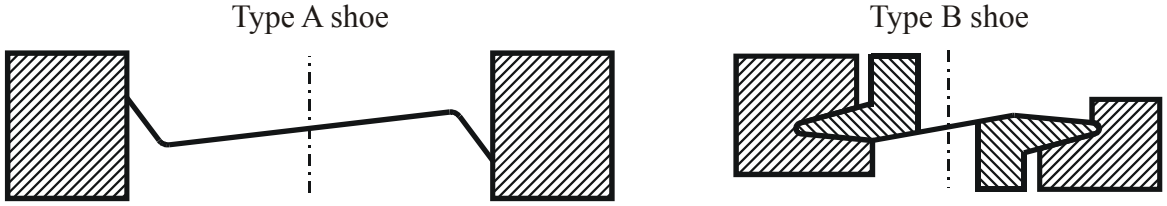

Fig. 10. Forming shoes for edge waves reduction [40].

The fundamental study of edge waves appearing within the CRF process carried out by Kimura [40] for forming a painted aluminium strip into the S-profile section showed that the forming shoes (see fig. 10) installed between forming roll stands can reduce:

1) the final height of the edge waves by approximately 95%;
2) the edge waves existing on coils by approximately 97%.

When the formed strip passed through the forming shoes of the cross-sections shown in fig. 10, its edges were subjected to additional plastic deformation by the shoes, reducing the edge wave effect in Kimura's experiments [40].

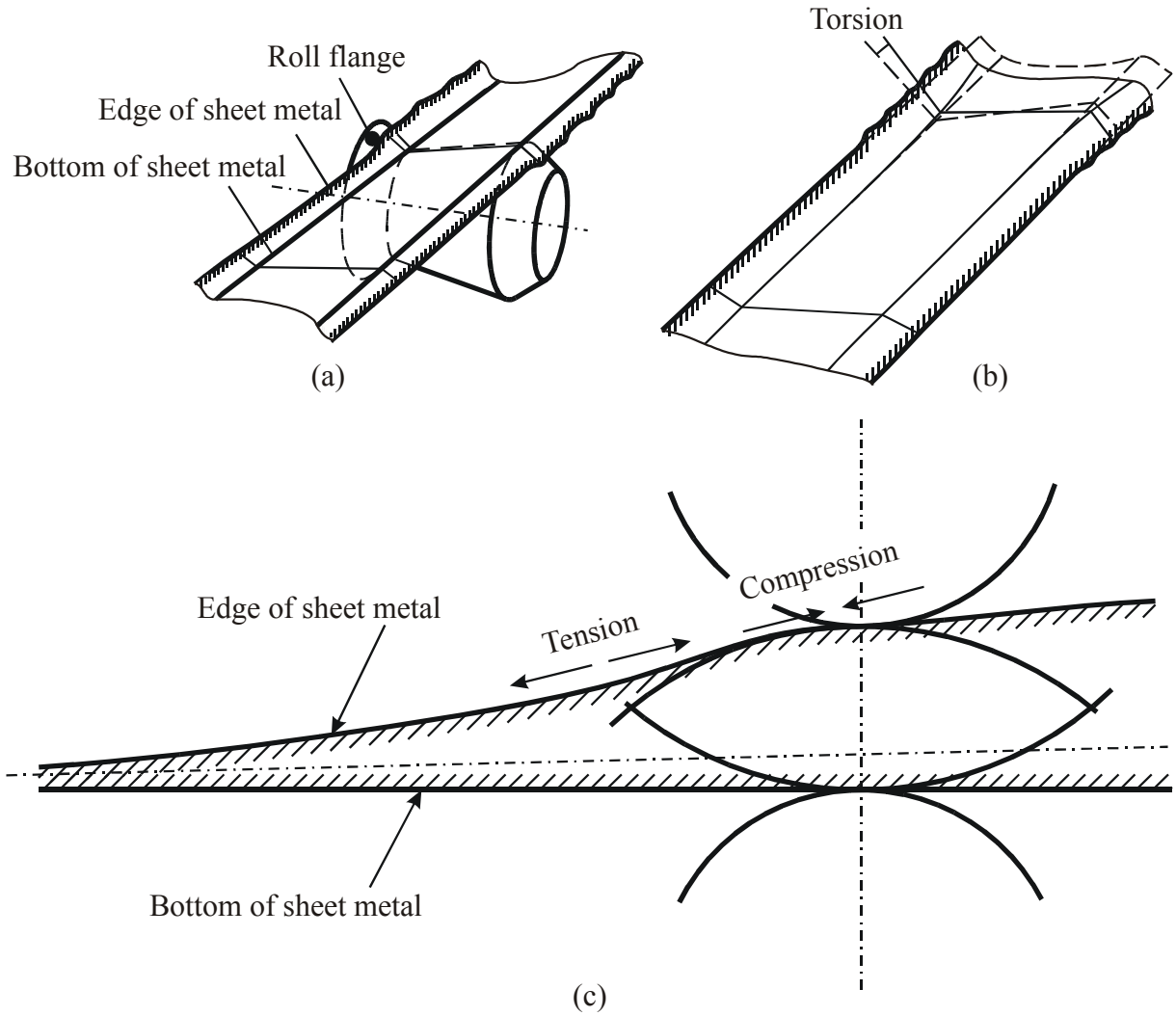

Fig. 11. Edge waves on S-type profile caused by (a) bending, (b) torsion, (c) compression [40].

Kimura [40] established also, that:

1) the height of edge waves scatters in its value even if the same forming conditions are maintained;
2) the edge waves are the result of either bending, compression or torsion of the strip within the CRF process (see fig. 11).

The edge waves (due to strip buckling in the edge regions of the formed strip) are caused by the maldistribution of the longitudinal plastic strains across the strip, where the edges are overstretched by unfit rolls, (fig. 11 (a)) during the CRF process (tension area in fig. 11 (c)) and subjected to the compression from the side of the less stretched regions of the strip (compression area in fig. 11 (c)). The maldistribution of longitudinal plastic strains may result not only in the edge wave effect, but also in bending and torsion shown in fig. 11 (a), (b).

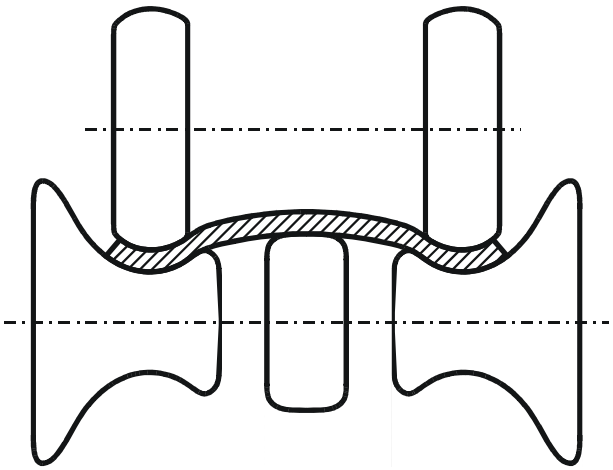

Fig. 12. Double bending method [44].

Okamura and Takada [65] proposed avoiding edge waves using a "double bending method", when both the edges of the sheet are bent to the desired shape with ω-type profile rolls of double calibres, at the initial stage of the forming process (fig. 12).

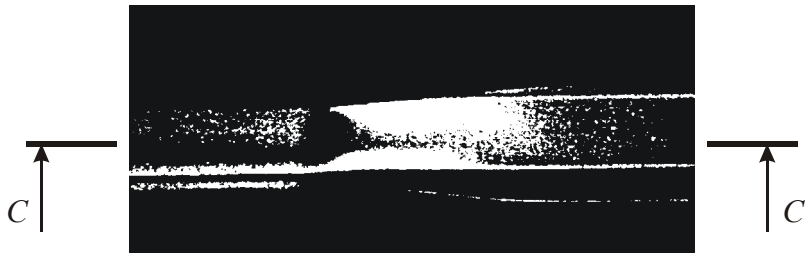

(a) A slight buckle

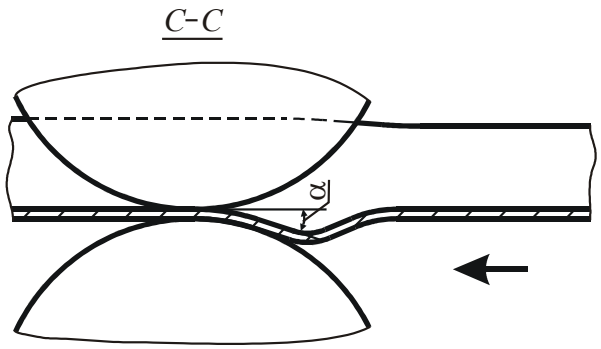

(b) C-C section of the slight buckle

Fig. 13. A slight buckle on the web part in front of each roll stand [37].

Jimma and Ona [37, 66 – 71] found that slight buckling at the web of a channel profile, the so called pocket waves or oil canning before the forming roll at each station, indicates the severity of forming (see fig. 13 (a)). This slight buckle looks like the pocket wave, but it grows just in front of the rolls and disappears soon after passing the rolls [37]. As the magnitude of the slight buckle was found to be strongly related to the severity of forming at the roll stand, the severity of forming was evaluated via inlet angle of the centre line on the waved part (see fig. 13 (b)) [37]. Jimma and Ona showed in the experiment, that the edge waves appear when the buckle inlet angle exceeds 4° (see fig. 14) [37]. They noted that the slight tension of the strip at the final pass could prevent edge wave formation.

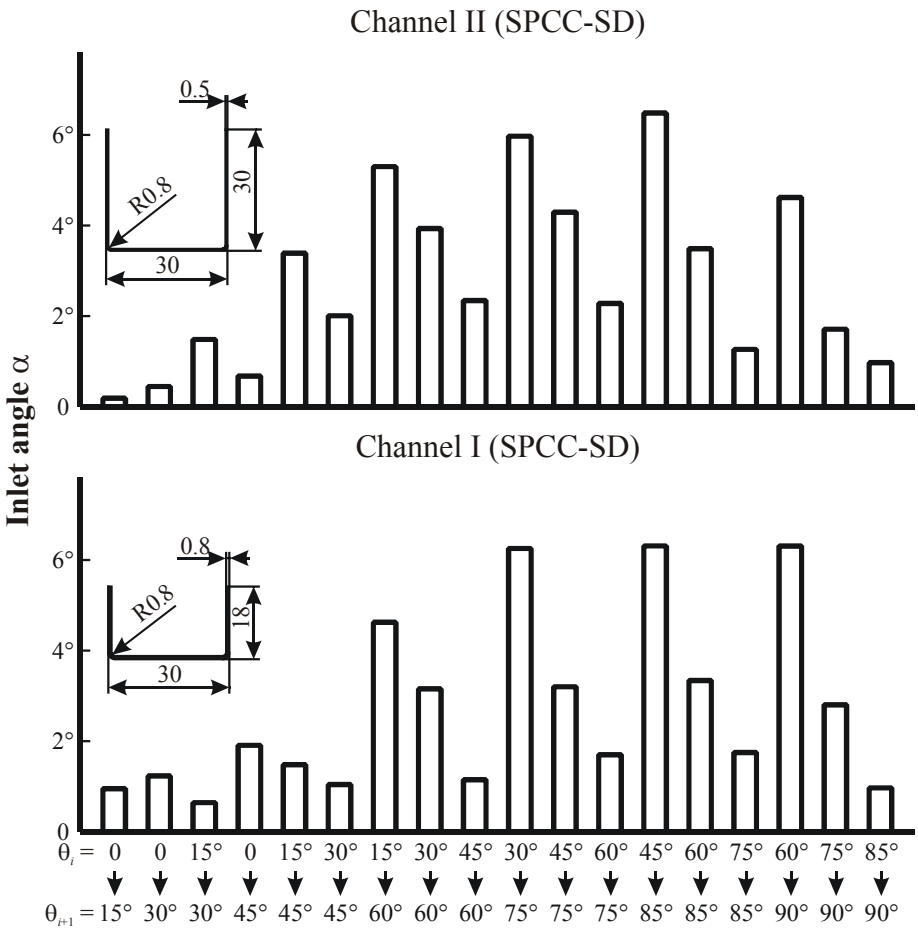

Fig. 14. Inlet angle of the centre line of the web part during forming from bend angle θ_i to θ_{i+1} [37].

Chiang [18] showed that the edge waves can be a result of longitudinal bending of the formed profile which was also confirmed in later numerical simulation by Farzin et al [22].

The experiments [20, 29, 30] showed that the formation of edge waves depends on strip thickness and formed flange length.

Wen and Pick proposed a numerical model for predicting edge instabilities in ABAQUS [104]. They analysed the influence of different forming parameters on edge stability, but provided no comparison of the numerical results with the experimental data, which significantly depreciates their work.

Toyooka [88] proposed the pure theoretical approach to analysis of edge waves, but his results were not correct because he made many rough simplifying assumptions.

2.2.4. Pocket waves

Hira et al [31] studied the effect of formed material properties on pocket waves formation in CRF of siding board. They showed that the higher yield stress, or the smaller Poisson's ratio at upper yield point, or larger yield elongation is then the smaller pocket waves are formed.

As a general method of avoiding pocket waves formation Hayashi and Takatany proposed adjusting stress-strain relationship, strain hardening and yield elongation of the strip to reach more uniform stress and strain distributions in it [28].

Jimma and Ona proposed a shape factor [68] to evaluate the roll forming severity.

Miyamoto and Hawa [59] carried out the experimental research and developed a method of pocket wave severity measurement. They showed that the increase of the yield stress leads to decrease of pocket wave formation.

The pure theoretical analysis of strip instability phenomena by Tomito and Shao [87] produced qualitative results, but the current state of shell theory does not (allow performing the formed strip instability analysis with the accuracy necessary for the CRF process design).

The mechanism of pocket wave formation and the effect of mechanical properties on this process were also analysed in details by Nakako et al [64].

2.2.5. Corner Buckling (Herringbone Effect)

Localized longitudinal elongation tends to occur frequently at corner portions when products have rather wide cross-sections and the material is thin [26]. If the stiffness of the corner portions is comparatively low, when the elongated corner portions shrink in the longitudinal direction, at the exits of the roll gaps, buckling deformation takes place at the corners and adjacent areas [26]. This is a sort of plastic shear buckling when small waves appear periodically along the corners.

To prevent corner buckling similar precautions must be taken as in the case of pocket waves [26].

However this effect occurs rarely and no publications about its experimental investigations could be found at present time, as general recommendations for roll designers allow avoiding herringbone formation.

3. Phenomena affecting the CRF process

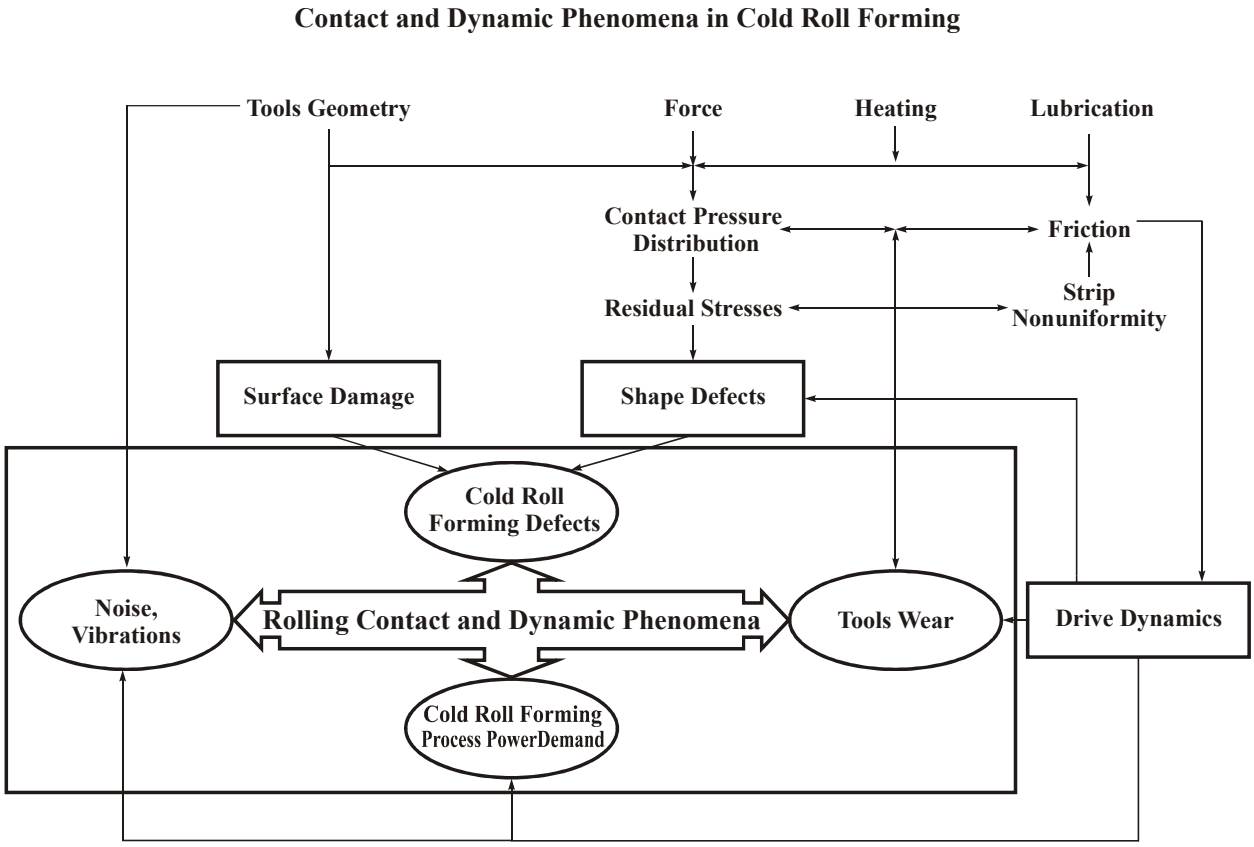

Fig. 15. *Phenomena related to contact and dynamic conditions in CRF*

The CRF process is accompanied by the series of interdependent phenomena related with rolling contact and mill dynamics (see fig. 15). These phenomena affect the quality and the cost of formed product. But, the existing CAD/CAM/CAE software for the CRF process does not provide a well-founded analysis of these effects even if they are taken into account due to lack of proven theoretical footing.

3.1. Strip non-uniformity

The strips for the CRF process are usually cut from cold or hot rolled steel sheets. The sheets have non-uniform material properties and thickness varying in longitudinal and transversal directions due to rolling technology conditions. The sheet non-uniformity causes variation of strip material properties and thickness in both directions. The strip surface properties vary along and across the strip piece too. The hot rolled strips have a rougher surface than the cold rolled strips of the same thickness. All strips have initial variations in plane flatness that are reduced using calenders in the preparatory mill stands.

The strip material property variation affects the CRF process. This reality was demonstrated by Brown [11] who studied strain distribution in CFR symmetrical trapezoidal profiles for three different work materials, but made no clear conclusion from the experiments. He was followed by Carson [16] and Boyens [10], who investigated strain distribution for various work materials, and found that residual strains and strains peak values varied significantly for different materials under the same forming conditions. Ding and Duncan [21] showed that temporal change of strip material properties could affect the spring-back.

However the accuracy of any strip material model must be reasonable and comply with the expected accuracy of the solution [90].

3.2. Dynamic phenomena

CRF is a complex dynamic process accompanied by a series of specific dynamic phenomena including:

1) dynamic loads;
2) power dissipation;
3) noise and vibrations generated by a diversity of sources.

All these phenomena influence the service life of CRF equipment, electric power consumption and strongly affect the CRF-mill shop environment, but are not well investigated and not taken into account in modern CAD software for the CRF process design.

3.2.1. Noise and vibrations

Noise and vibrations generated within the CRF process, influence CRF-mill shop environment and tool wear.

The sources of noise and vibrations generated during the CRF process include:

1) areas of material plastic deformation [108];
2) kinematic pairs of rolling or slipping contact where friction instability, geometry peculiarities or out-of-balance movement take place;
3) electric drive;
4) mechanisms performing auxiliary operations in a CRF-mill, such as flying shears, welding machine, systems for lubricoolant supply and recirculation etc.

The effects related to noise and vibrations are still not well investigated. As a rule these effects are considered as an undesirable incidental result of the CRF process that requires only safety protection measures to be taken. However, it could be more expedient to reduce the noise and vibrations originating from the sources, and to employ the effective dynamic suppression of equipment vibrations, but such approach inevitably requires the separate sophisticated process study and analysis.

3.2.2. Drive dynamics

The electric drive not only moves the strip in the CRF-mill, but excites vibrations with a number of harmonics. These vibrations could lead to large dynamic loads in the CRF-mill and decrease its service life [17].

The correct analysis of a CRF-mill drive dynamics carried out by Cherevik [17] facilitated improving the mill dynamic characteristics and decreasing its drive load variation factor from 1.8 through 2.2 to 1.3 through 1.5, thus reducing mill dynamic loads, which was confirmed with experimental research [17].

Although the improvement of mill dynamic characteristics promises quick and obvious affordability, the analysis of mill drive dynamics is a complex problem that is formulated rarely and is not incorporated in modern commercial software for the CRF process design.

3.2.3. Power losses

Power losses are closely related both with CRF-mill drive dynamics, the dynamic effects observed in the CRF process and with friction that takes place in mill kinematic pairs. Although power losses are related with tool wear directly, we could not find any publications concerning studies of this CRF phenomenon. Based on trends in other industries we can expect that power efficiency will become an important parameter considered in further development of CRF equipment. But taking power efficiency into account at the design stage, requires predictive theoretical

analysis and experimental investigations, including studies of CRF contact phenomena appearing in mill kinematic pairs, due to friction and wear.

The theoretical analysis and experimental investigations of contact phenomena, related with power losses caused by friction and wear, constitute a subject of further tribological research.

3.3. Contact phenomena

Contact phenomena occurring in CRF include:

1) friction and wear in the electric drive;
2) friction and wear of mechanisms transmitting the power from the electric drive to the mill;
3) friction and wear in auxiliaries;
4) friction and wear in bearings;
5) friction and wear in roll-strip contacts.

Contact phenomena occurring in the electric drive are usually taken into account in electric drive design. The power efficiency and the service life of the electric drive are usually known and recorded in a name plate of the drive.

The service life and power efficiency characteristics of mechanisms transmitting the power from the electric drive to the mill, are usually known too, as such mechanisms are standard.

Friction and wear in auxiliaries represent a separate problem complementary to friction and wear in the CRF process.

Friction and wear in roll bearings have a well established relation with the loads applied to the bearings, and thus depend on the roll forming forces that are calculated during the CRF process design.

Friction and wear in roll-strip contact affect not only the CRF process energy efficiency, but have a strong effect on roll service life and therefore on the CRF mill down time. The friction in roll-strip contact depends on contact geometry, contact stress distribution and presence of lubricant in the contact area. The wear of the roll depends on roll surface hardness, the friction coefficient in roll-strip contact area and the contact pressure distribution.

In spite of a great progress in tribology that took place in the last decades, the effects of friction and wear in the CRF process are still not widely researched, even though CRF tool wear is costly.

3.3.1. Contact pressure distribution

The roll-strip contact pressure distribution has been impossible to measure during the CRF process until present time. The theoretical study of roll-strip contact pressure distribution is a complicated problem that has not been solved yet. The roll-strip contact pressure is estimated via approximate models, and is validated by loads measured on the forming rolls. These approximate roll-strip contact pressure distribution models were developed on the basis of experimental investigations.

Two approaches were used for experimental investigations of contact pressure distribution in a roll-strip contact (see table 1).

Table 1. An investigation into roll-strip contact pressure distribution.

Approach 1 [38]	**Approach 2 [85]**
1. Direction of contact force linear distribution measurement	
Along the strip	Across the strip
2. Assumed model of roll-strip contact pressure distribution	
Linear distribution across the strip	Sinusoidal distribution along the strip

The first approach to investigation into roll-strip contact pressure distribution was proposed by Kato [38] in 1963. At the first stage of his work Kato performed series of experiments with three pairs of mated rolls shaped for 30°, 60 and 90 bending of 0.5 × 8 mm strips into a (3 × × 3 × 0.5) mm channel profile (see fig. 16) to study the forces acting during the CRF process. He compared dynamic roll forming load, measured during the CRF process with results of a roll press test, where the forming rolls were not rotated, but used to press the strip of an indefinite length, inserted up to the central plane or narrowest point, in the clearance between upper and lower rolls. Results of this test for the strip of 0.5 mm thickness are shown in fig. 17 (a). The sharp rise of each curve corresponds in fig. 5 to the point where the rolls begin compressing the strip [38]. The measured dynamic load is compared with the result of the roll press test in fig. 17 (b), where strip A thickness is 0.51 mm and strip B thickness is 0.53 mm.

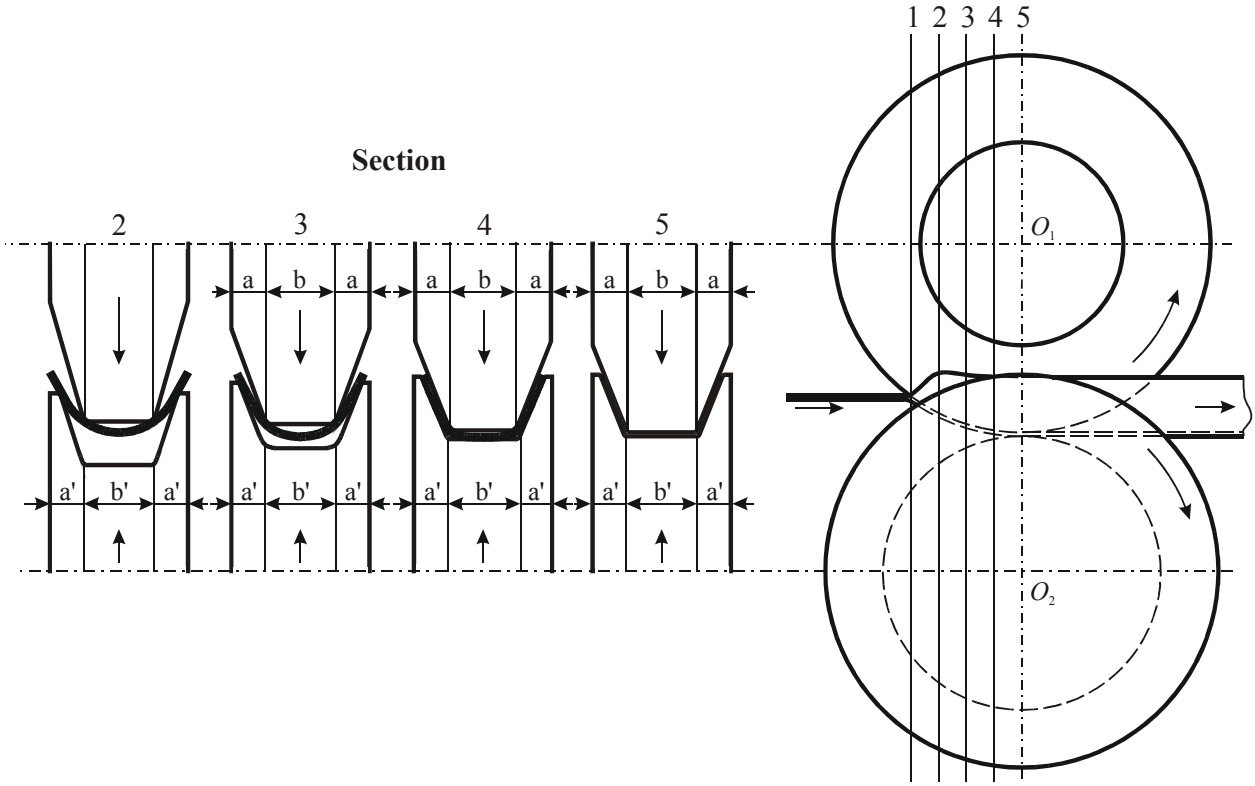

Fig. 16. CRF of channel profile [38].

The difference between static and dynamic loads was not large in Kato's experiments [38] as the experiments were carried out for the comparatively small rotation speed of only 60 rpm.

The effect of roll clearance on forming load was studied by Kato [38] for the CRF process of channel section shown in fig. 16 (from 0.51 mm thick and 8 mm wide strip with varied roll clearances). Obtained [38] forming load dependence on clearance is shown in fig. 18 (a). The large variance between dynamic and static forming loads for 90 bending was explained by Kato by the influence of friction, that was greater in the dynamic test than in the roll press test [38].

Kato observed the correlation between the forming load components, roll torque and drawing force (see fig. 18 (b)), where drawing force is the force required for drawing the strip between the rolls in the roll press test [38].

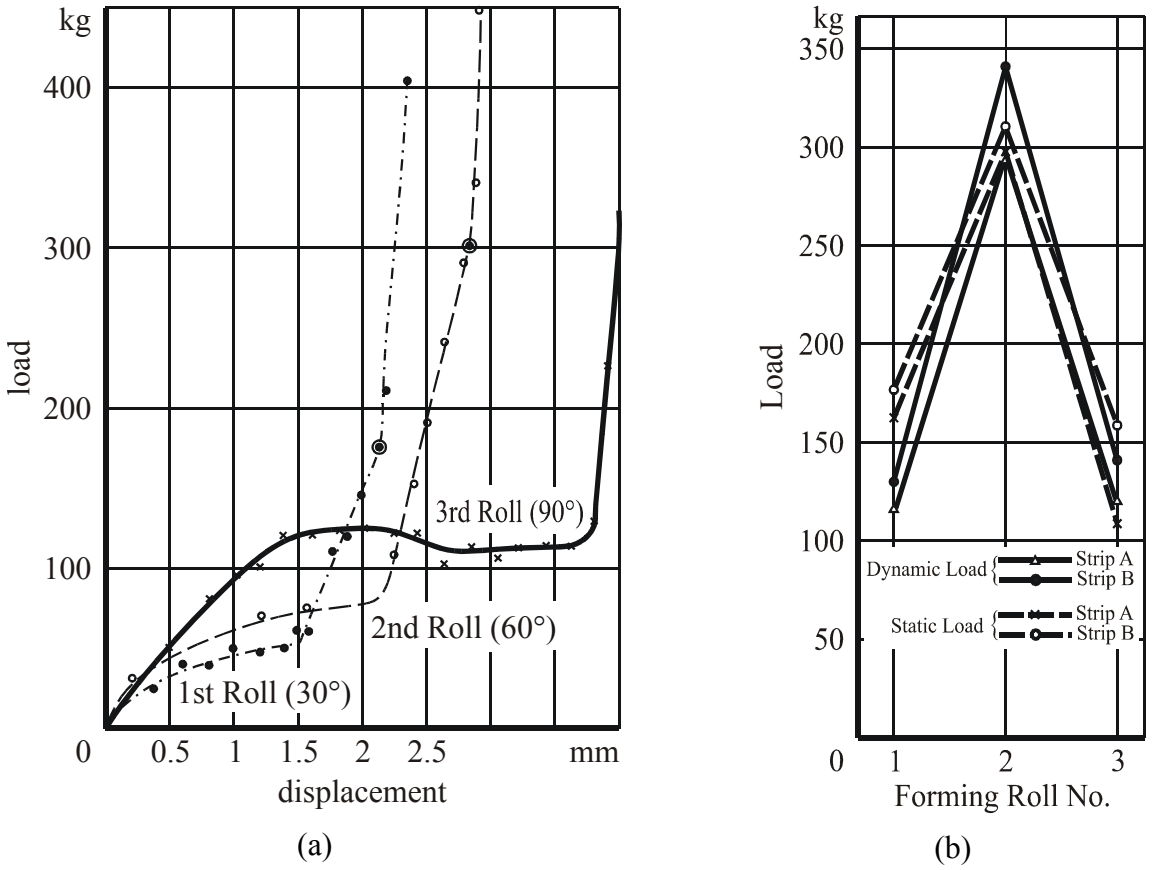

Fig. 17. Roll press test result (a) and CRF dynamic load (b) [38].

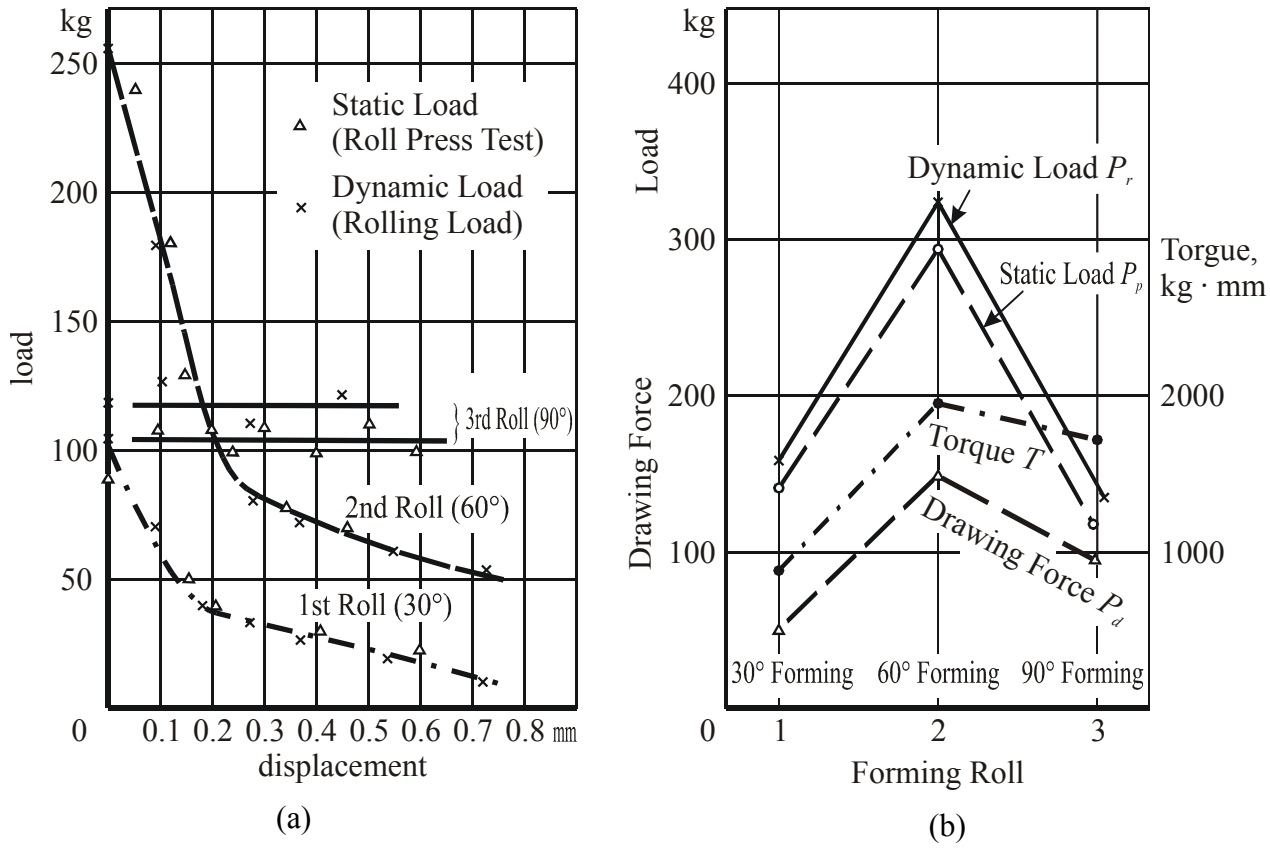

Fig. 18. Relation between forming load and roll clearance (a) and between dynamic load, static load, roll torque and drawing force (b) [38].

The data about the effective forces obtained during CRF of a channel profile allowed Kato to propose the first simple model of contact pressure distribution (fig. 19).

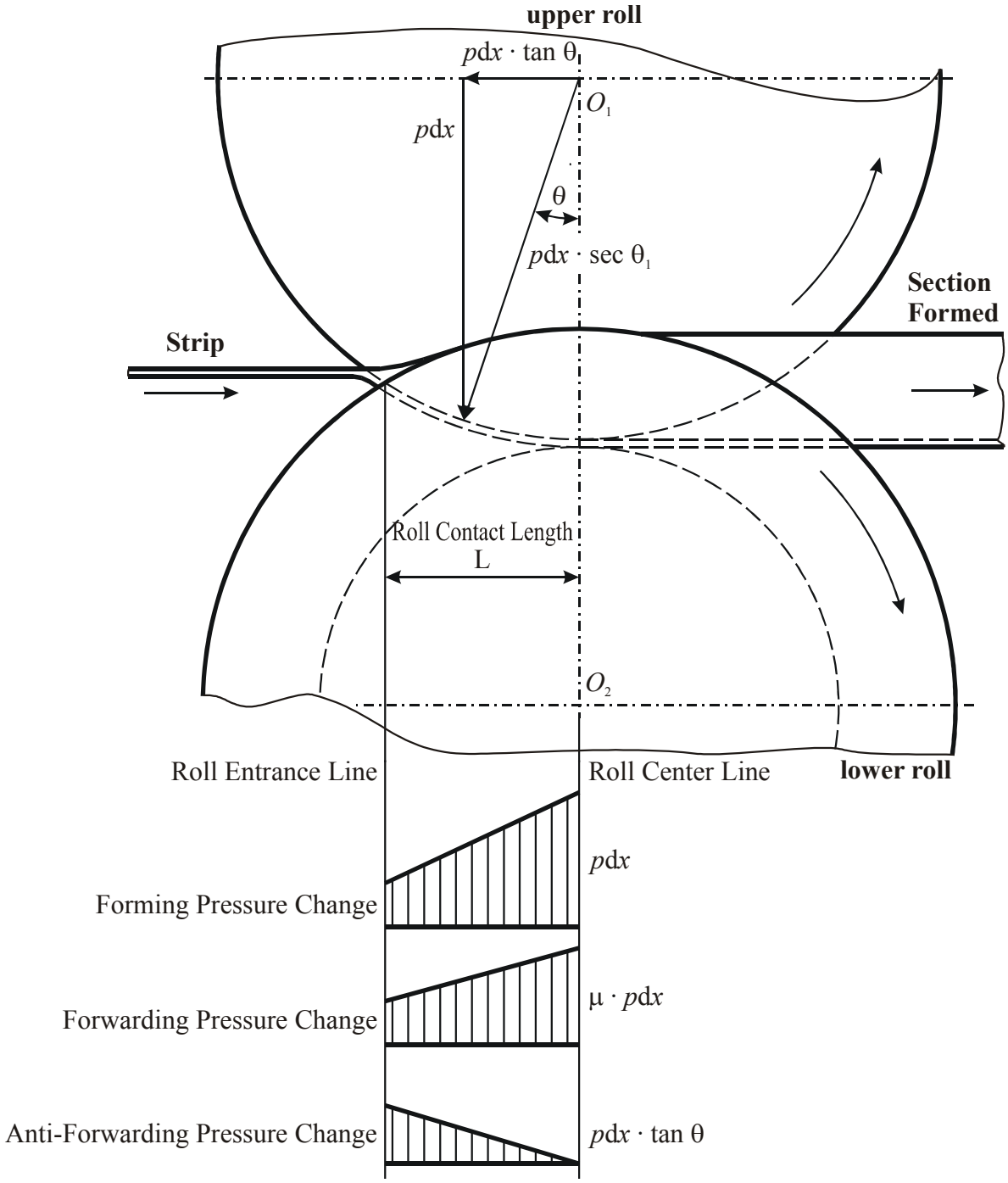

Fig. 19. Pressure distribution in roll-strip contact during the CRF process [38].

The force acting in the roll-strip contact during the CRF process was decomposed into radial and propelling or forwarding components (fig. 19) [38]. The radial component was represented as a sum of bending force and retarding or anti-forwarding force [38]. Kato [38] assumed that the forming pressure is proportional to the roll contact length, L, that he proposed to calculate from geometrical conditions (fig. 20) by the formula (1):

$$L = \frac{1}{2 \cdot R} \cdot \sqrt{R^2 \cdot \left(2 \cdot r_1^2 + 2 \cdot r_2^2 - R^2\right) - \left(r_1^2 - r_2^2\right)^2}\,, \tag{1}$$

where R is the distance between rolls centres;
r_1 is the convex roll radius;
r_2 is the concave roll radius.

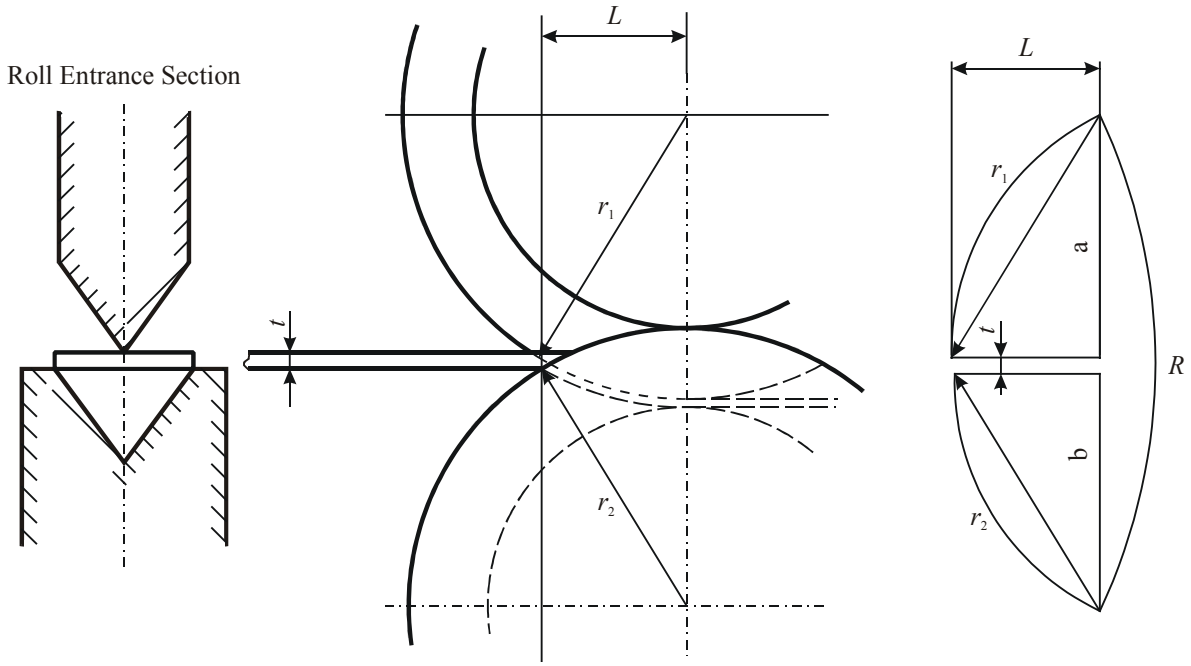

Fig. 20. Roll contact length [38].

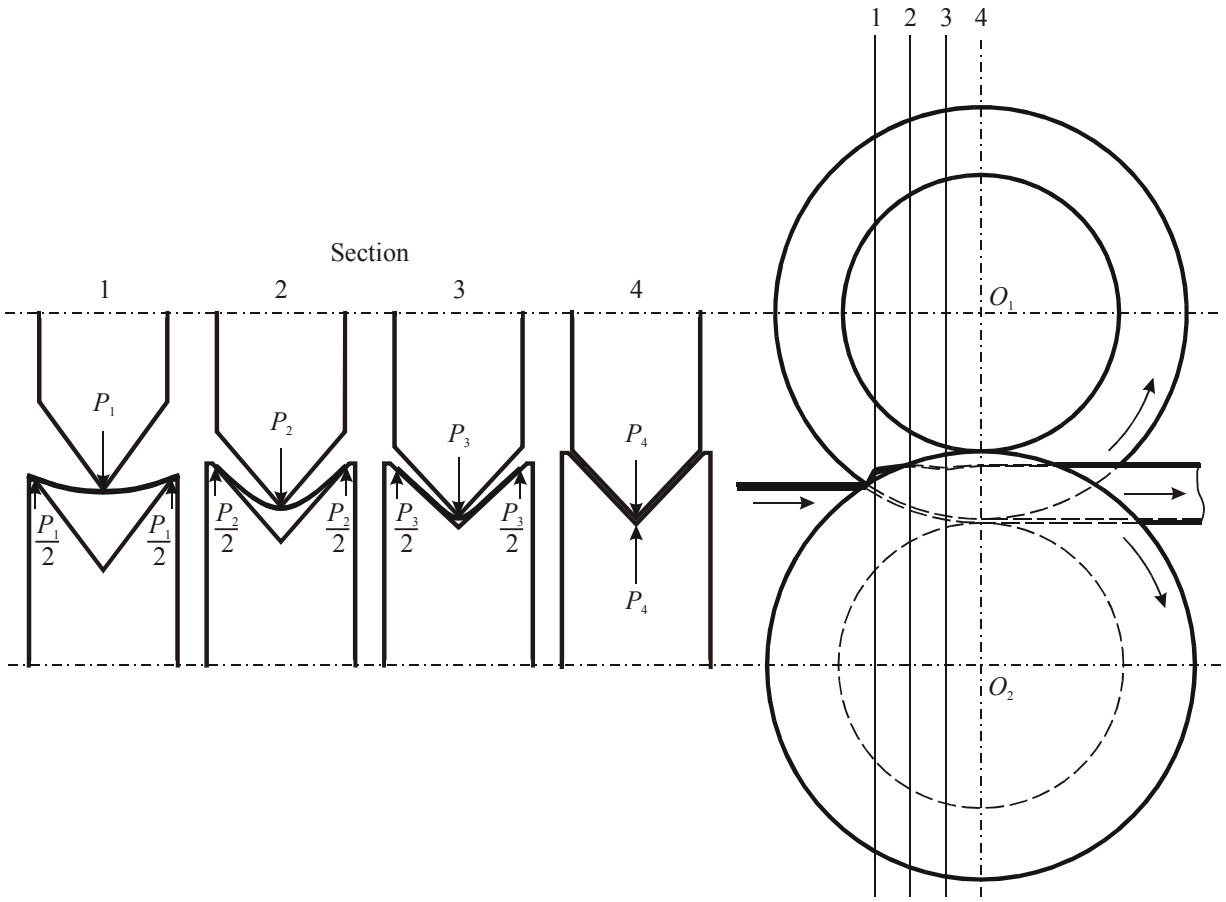

Fig. 21. CRF of angle profile [38].

Kato made the first attempt of direct measurement of roll-strip contact force distribution for an angle section for angle section (see fig. 21) using a simple measuring apparatus shown in fig. 22 for this work [38].

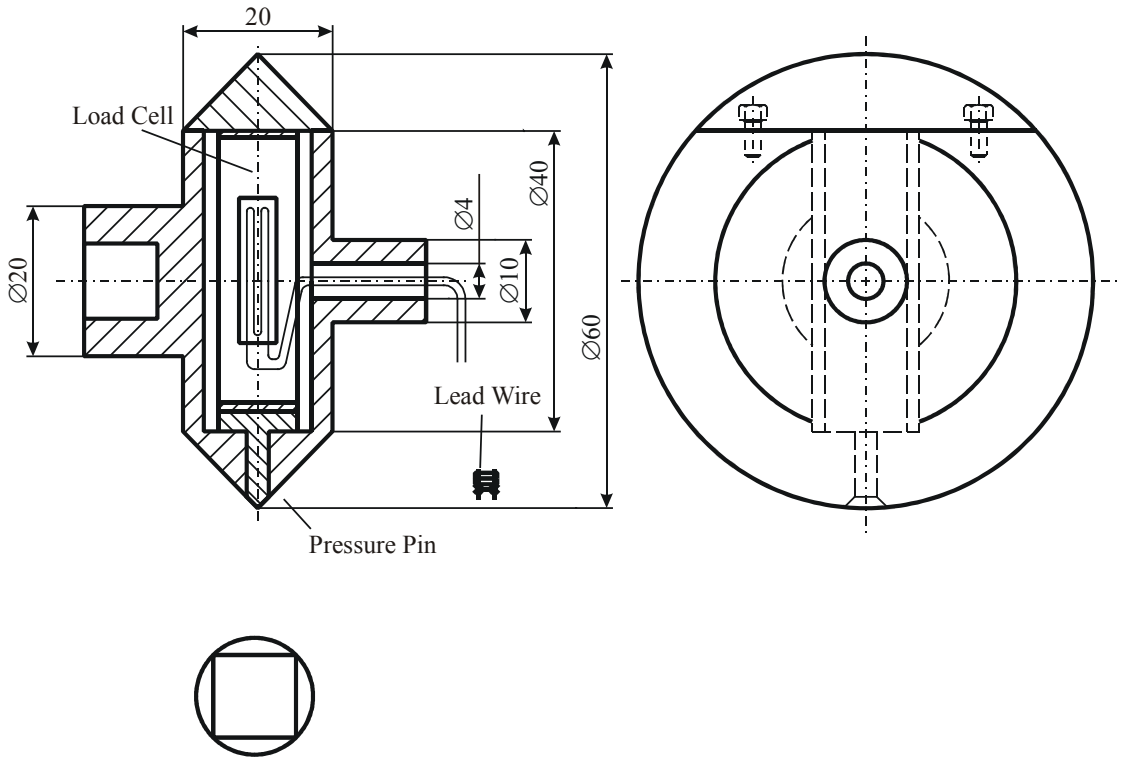

Fig. 22. Apparatus for measuring roll-strip contact force distribution [38].

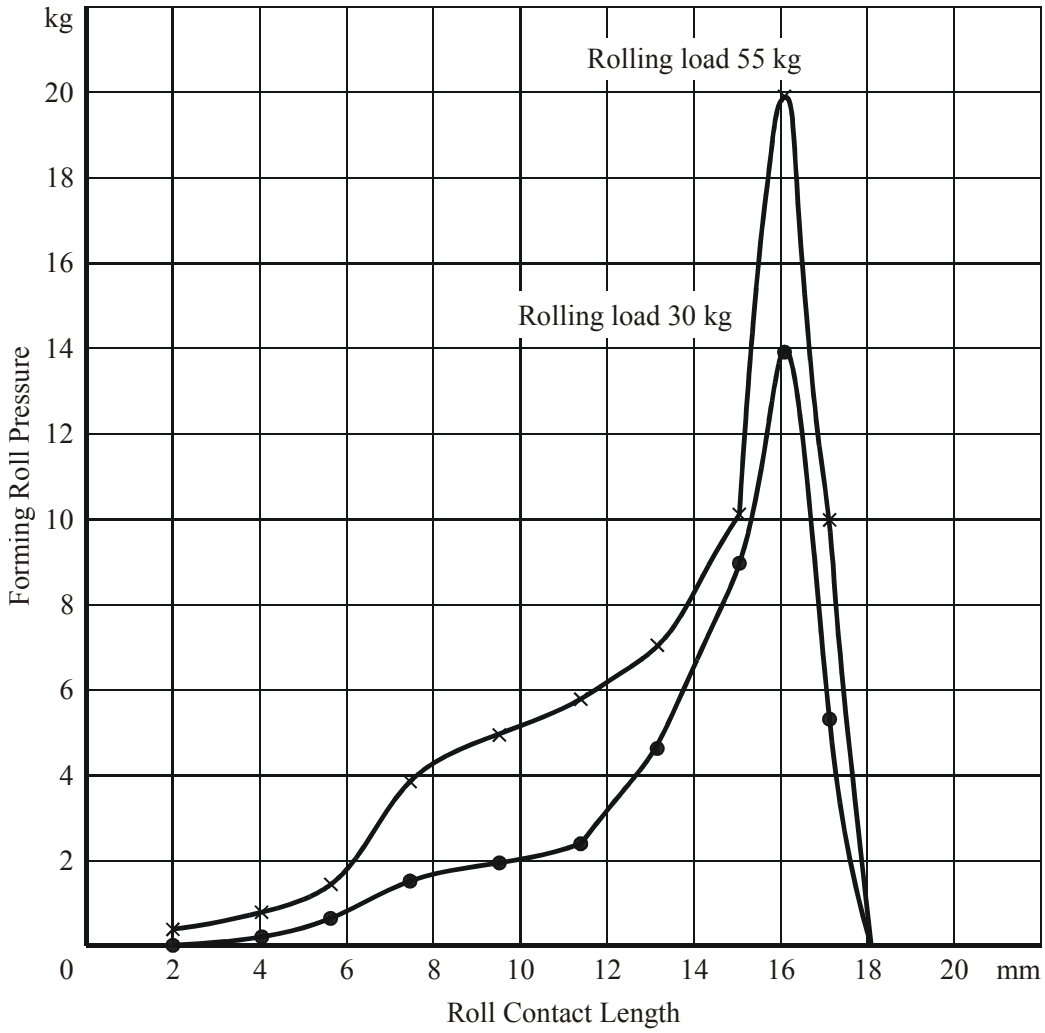

Fig. 23. Roll-strip contact force distribution during the CRF process [38].

The pin load was measured for bending a strip with 55 kg (540 N) and 30 kg (294 N) forming load (see fig. 23) [38]. The roll-strip contact length (fig. 23) was measured for the roll peripheral length corrected for the diameter of the pressure pin [38]. The measured roll-strip contact length coincided with the value calculated by the formula (1) within the accuracy of 2.5% in Kato's experiment [38].

The accuracy check of contact pressure distribution model includes the comparisons between:

1) the forming load calculated from the model and its measured value;
2) the roll torque calculated from the model and its measured value.

The summation of the measured values of force in the roll-strip contact points (fig. 23) gives 53 kg (520 N) where the actual load was 55 kg (540 N) that corresponds with 3.6% error, and 28 kg (275 N), where the actual load was 30 kg (294 N), that is within 6.7% error [38]. The error of a roll torque value calculated from Kato's model of contact pressure distribution was found to be less than 40% for 30° bending and less than 51% for 90° bending [38]. The error was explained with the expected friction effect [38].

The weakness of Kato's approach to contact pressure gaging was that he did not consider the real roll-strip contact geometry and did not study the forces acting both in concave and convex rolls, forming the same profile.

The strength of Kato's approach was that the pin contact force was measured directly with a relatively small experimental error for the considered V-type profile forming.

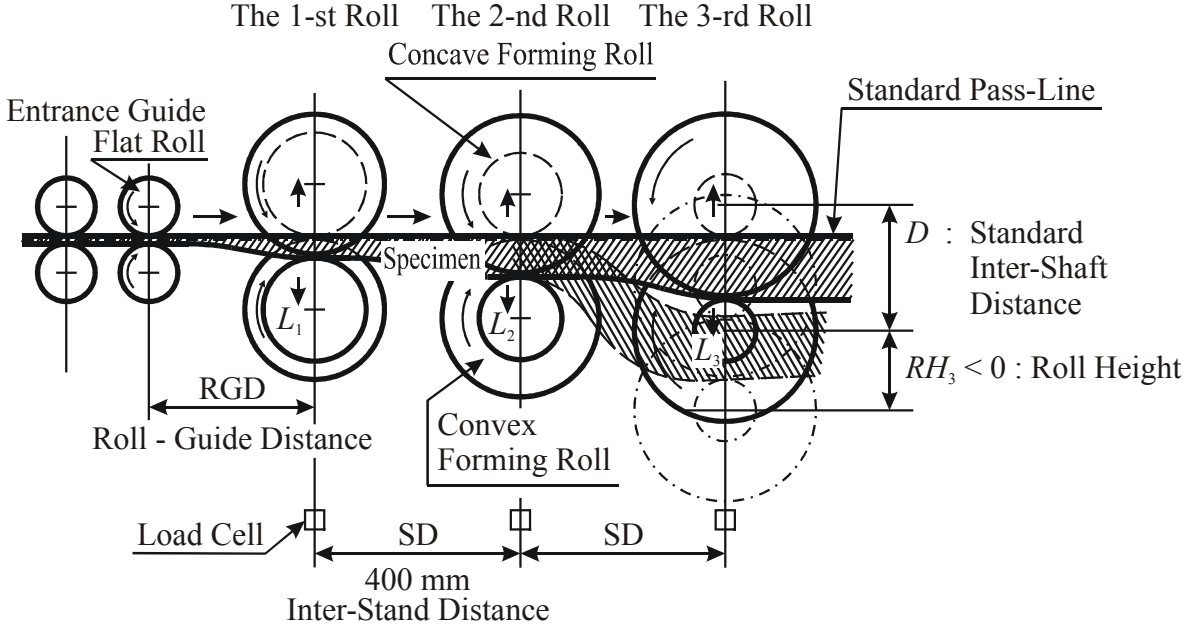

Fig. 24. Schematic diagram for CRF through tandem mills [85].

The later study of contact pressure distribution was performed by Suzuki et al [85] for CRF circular, trapezoidal and V-type grooves using the forming machine comprised of tandem mills (fig. 24) [85]. The forming rolls (fig. 25) were installed in 7 different pas-lines (fig. 26) to reveal the influence of the rolls positional relationship on roll-strip contact face and contact pressure distribution [85].

Rolls with the desired roll clearance RC equal to the strip thickness were put in along the considered pass-line and the strip coated with a thin layer of forming oil, (water-soluble cooling oil), was fed into the rolls and formed, and the forming machine was stopped when the top part of the strip reached the exit side of third roll stand, to establish the roll-strip contact face [85]. Fine powder (wheat flour with a grain size of 20 μm or less) was fully blown against the specimen with compressed air (4 $\frac{kg}{cm^2}$ (0.39 MPa) or 6 $\frac{kg}{cm^2}$ (0.59 MPa)) from the entrance and exit sides of the rolls, and then the strip was removed by lifting the upper rolls to measure the region of contact between rolls and strip [85].

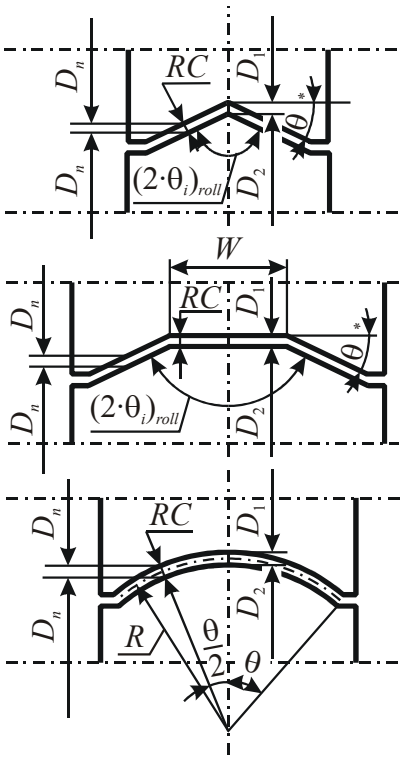

	θ*, °	D_1	D_2	D_n	RC			
#1	15	202.5	179.1	191.0	1.5	2.3	3.0	3.8
#2	30	215.0	167.0	191.0	1.5	2.3	3.0	3.8
#3	45	225.0	156.0	191.0	1.5	2.3	3.0	3.8

	θ*, °	D_1	D_2	D_n	RC				W
#1	15	202.5	179.1	191.0	1.5	2.3	3.0	3.8	60
#2	30	215.0	167.0	191.0	1.5	2.3	3.0	3.8	60
#3	45	225.0	156.0	191.0	1.5	2.3	3.0	3.8	60

	θ, °	R	RC	R_n	R_1	R_2
#1	30	180	3.0	121	114.81	127.08
#2	60	70	3.0	121	108.74	132.86
#3	90	60	3.0	121	102.98	138.13

	θ, °	R	RC	R_n	R_1	R_2
#1	30	180	3.8	121	114.41	126.68
#2	60	90	3.8	121	108.34	132.46
#3	90	60	3.8	121	102.54	137.73

Fig. 25. Geometrical shape and dimensions of forming rolls [85].

Procedure of pass-line is denoted as *RH*(*a*, *b*, *c*)
Here, a = roll height in 1st stand
b = roll height in 2nd stand
c = roll height in 3rd stand

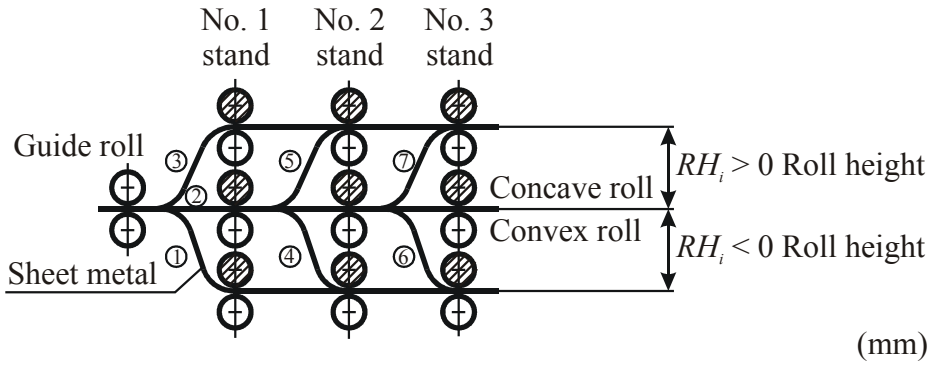

(mm)

Stand No. \ Pass-line No.		①	②	③	④	⑤	⑥	⑦
Forming process of product with circular arc cross-section	# 1	-16	0	44	0	0	0	0
	# 2	-16	0	44	-16	44	0	0
	# 3	-16	0	44	-16	44	-16	44
Forming process of product with V-type or trapezoidal cross-section	# 1	-20	0	30	0	0	0	0
	# 2	-20	0	30	-20	30	0	0
	# 3	-20	0	30	-20	30	-20	30

Fig. 26. Dimension of roll height RH_i in pass-lines [85].

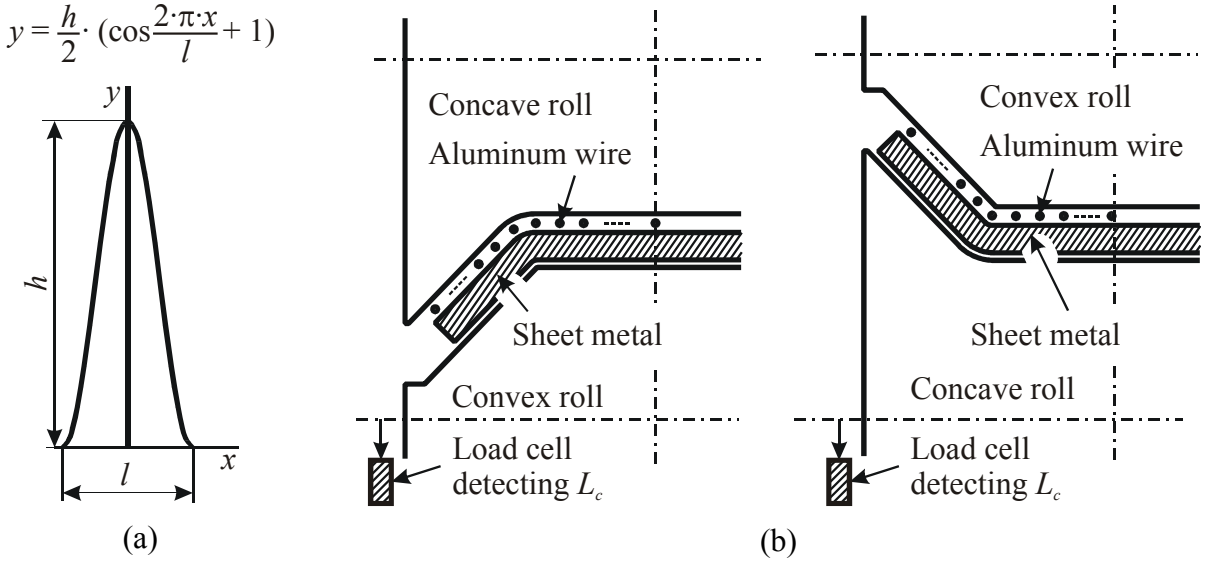

Fig. 27. Contact force longitudinal distribution model (a), specimen, stuck aluminium wires and load cells to measure the forming force and its transversal distribution (b) [85].

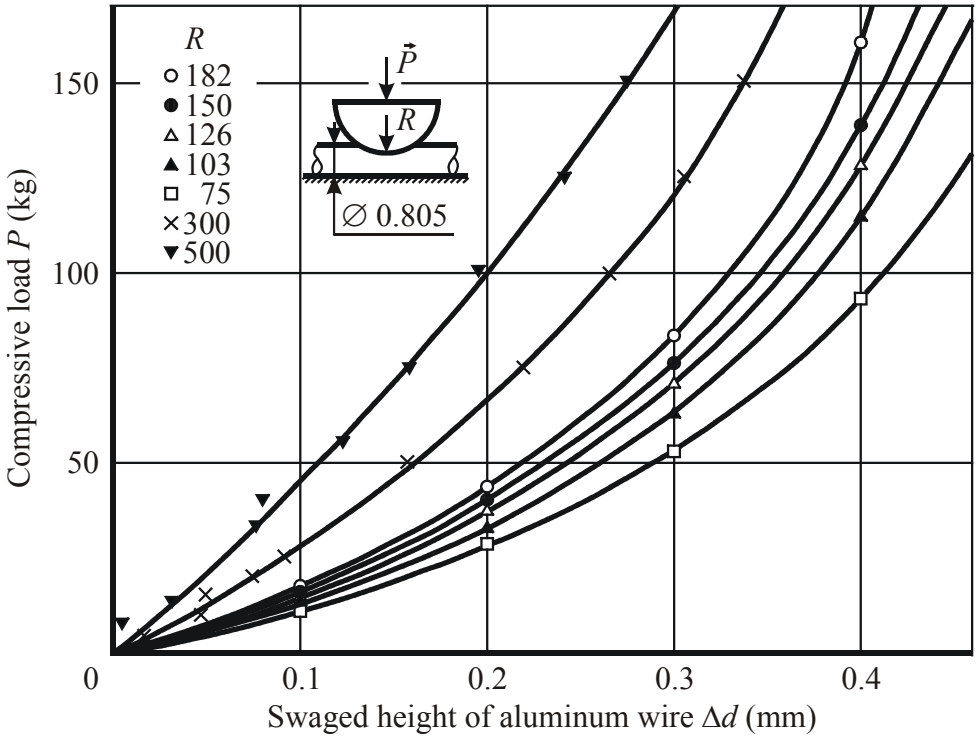

Fig. 28. Effect of the depth of indentation on compressive load P when aluminium wire was swaged with semicylindrical die [85].

The second approach to study of roll-strip contact pressure distribution was proposed by Suzuki et al [85] who measured the contact force distribution across the strip and proposed the approximate model for the contact pressure distribution along the strip within the roll-strip contact face (fig. 27 (a)), where h was found from maximum contact force measured in considered section of roll-strip contact face, l was a measured length of considered section of roll-strip contact face. The maximum contact force was measured by compression of annealed aluminium wires (∅0.805 mm × 50 mm length) placed along the formed strip, in considered sections of roll-strip contact face [85]. The roll forming was done with the forming rolls of the designed roll clearance RC (RC = strip thickness + diameter of aluminium wire) between them, until the top of the strip reaches the exit side of the third stand [85]. The forming machine was stopped

under this state and the prepared aluminium wires were stuck on the upper strip surface (89 wires were arranged in parallel at 2 mm intervals on the strip of 180 mm width as shown in fig. 27 (b)), with near and far ends of each wire fastened and annealed aluminium sheet 0.8 × 180 mm (sheet thickness × sheet width) put on the upper strip surface, before and after the stuck wires, to avoid the impact during rolling when the wires were rolled in. Then the forming machine was restarted and the compressed wires were removed after having passed the stands, to measure the depth of indentation that was compared with a correction curve (fig. 28). The correction curve was obtained from the separate experiment, where the wires were compressed with the semicylindrical dies of different curvature radii R, by the Amsler testing machine (fig. 29 (a)). As the wire was compressed during CRF as shown in fig. 29 (b), the load required as compared with the some depth of indentation, was considered to be about 0.5 of the value from the correction curve (fig. 28), when was proven by the separate compression test, by setting the end of the wire directly under the axial centre [85].

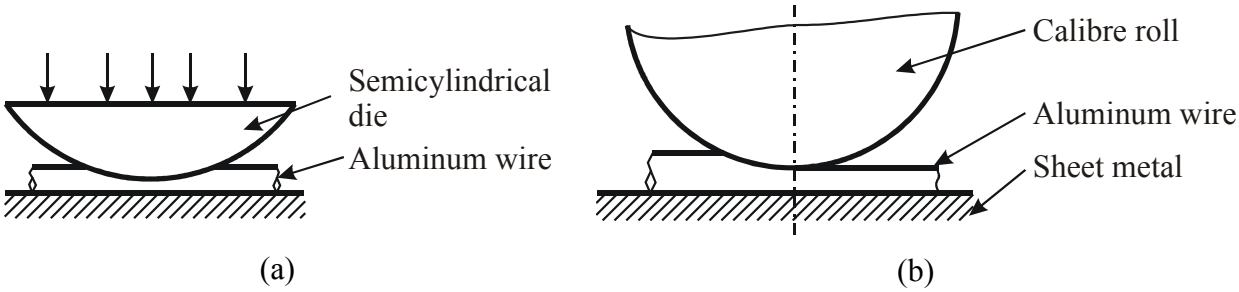

Fig. 29. Wire compressed with semicylindrical die (a) and wire inserted between calibre roll and sheet metal [85].

Suzuki et al [85] obtained the typical contact pressure distribution for forming circular, trapezoidal and V-type profiles from a strip of thickness t and width $2 \cdot b$ (fig. 30, 31, 32). The revealed contact pressure distribution is very non-uniform during the CRF process, both across and along the formed strip of all examined profiles [85]. The contact pressure was more uniform on the convex circular roll, while forming through the pass-line no. 7 and it had pronounced peaks at the bending areas of V-type and trapezoidal profiles [85]. Suzuki et al [85] analysed the effect of a number of annealed aluminium ∅0.805 mm wires, stuck at the intervals of 2, 3, 5 and 10 mm, in each position of sheet metal, in its transversal direction on the measured load, and did not find measurable effects of the intervals of wires sticking. But the examined 2 mm interval required more accurate measurements.

The effect of roll clearance increase during the experiment, on contact load distribution was considered very small for a circular profile (from 0 to 0.3 mm) and significant (more than 50% of wire diameter) but strictly localized, for trapezoidal and V-type profiles [85]. Although the error of forming load calculated value was up to 58% compared with the forming load measured using load cell during forming circular arc profile, through the pass-line no. 3, the calculated forming load was found to be compatible with the measured value for circular arc profile forming, through the pass-line 2 (error less than 30.5%) and pass-line no. 7 (error less than 37.1%) [85]. Suzuki et al [85] did not provide the data to estimate the error of forming load calculation for the trapezoidal and V-type profile forming, but noticed that this error was large. However the measured error could be significant for the wires compressed under pressure of 400 MPa … 1 GPa, taking into account the effect of friction and sizing tool instrumental error.

Suzuki et al [85] used the measured roll torque to check the accuracy of the contact pressure distribution model by calculation of a friction coefficient in roll-strip contact, as a ratio between the measured and calculated roll torque, and found the friction coefficient to have nearly appropriate calculated value, mostly within a constant range from 0.14 to 0.19.

Suzuki et al [85] also showed that the roll-strip contact face has a fractal nature (fig. 30, 31, 32, 33). However, the method used in the research [85] could not reveal the peculiar properties of the contact zone along the strip.

The calculated distribution of the force acting in contact between the top of the convex roll and the strip during forming V-type profile, using Suzuki's et al [85] model, radically contradicts the distribution built using Kato's experimental data (fig. 23) [38].

The rough approximation of contact pressure distribution is not the only irreducible error of Suzuki's et al [85] approach. The large compression of wires leads to an increase of transversal bending radius and decrease of forming loads during CRF trapezoidal and V-type profile, and changes roll-strip contact pressure transversal distribution. So, the contact load decreased at the top of V-type forming rolls on about 30% due to large plastic deformation of wires during CRF in Suzuki's et al experiment [85].

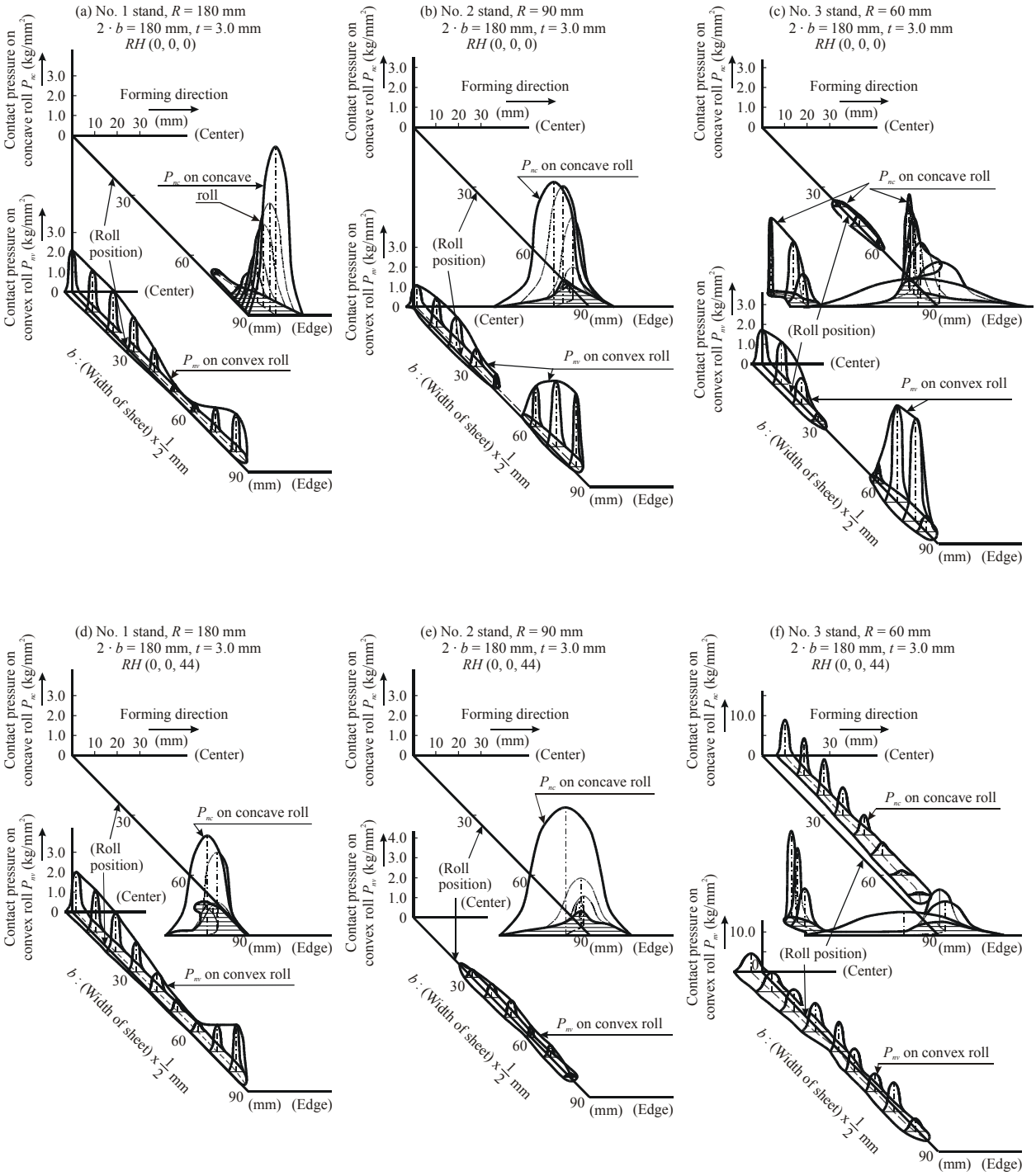

Fig. 30. Roll-strip contact pressure distribution in range from centre to edge of the strip; with contact pressure P_{nv} on convex roll and P_{nc} on concave roll during CRF circular profile [85].

(a) No. 1 stand, $(2 \cdot \theta_1)_{roll} = 150°$, $2 \cdot b = 120$ mm, $t = 3.0$ mm, RH (0, 0, 0)

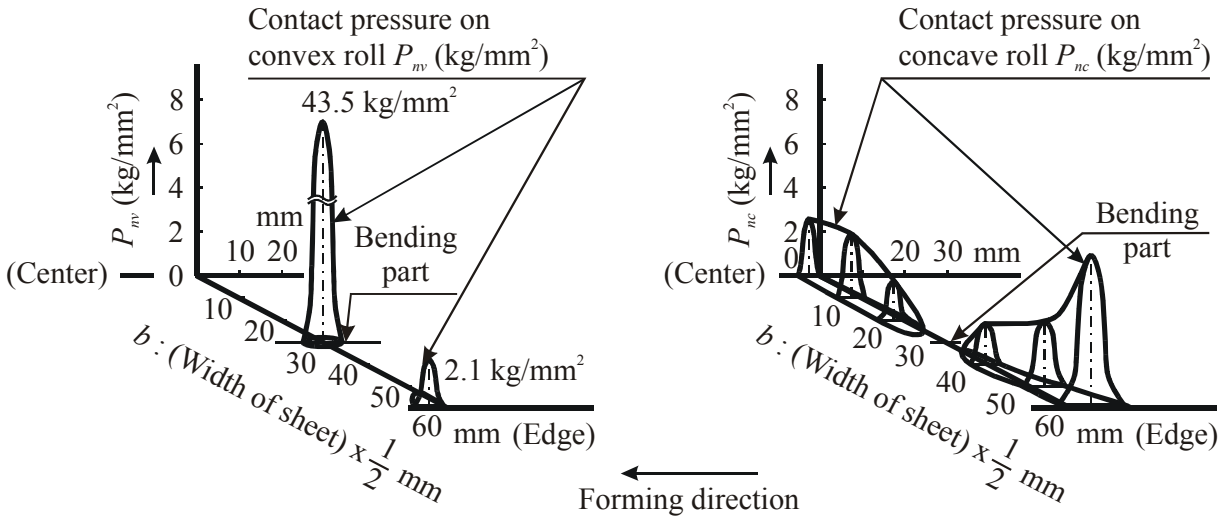

(b) No. 2 stand, $(2 \cdot \theta_2)_{roll} = 120°$, $2 \cdot b = 120$ mm, $t = 3.0$ mm, RH (0, 0, 0)

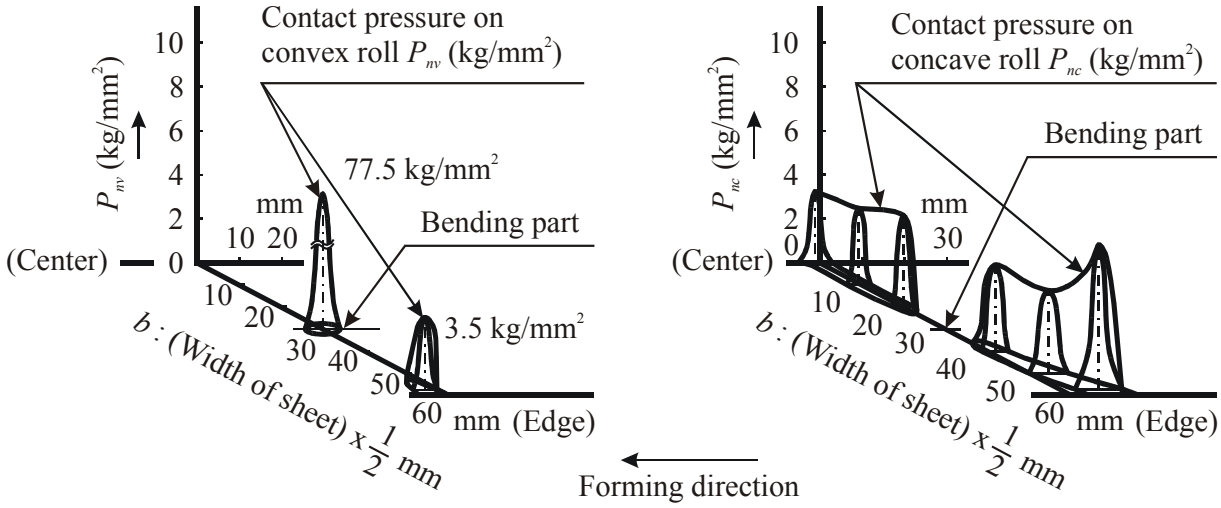

(c) No. 3 stand, $(2 \cdot \theta_3)_{roll} = 90°$, $2 \cdot b = 120$ mm, $t = 3.0$ mm, RH (0, 0, 0)

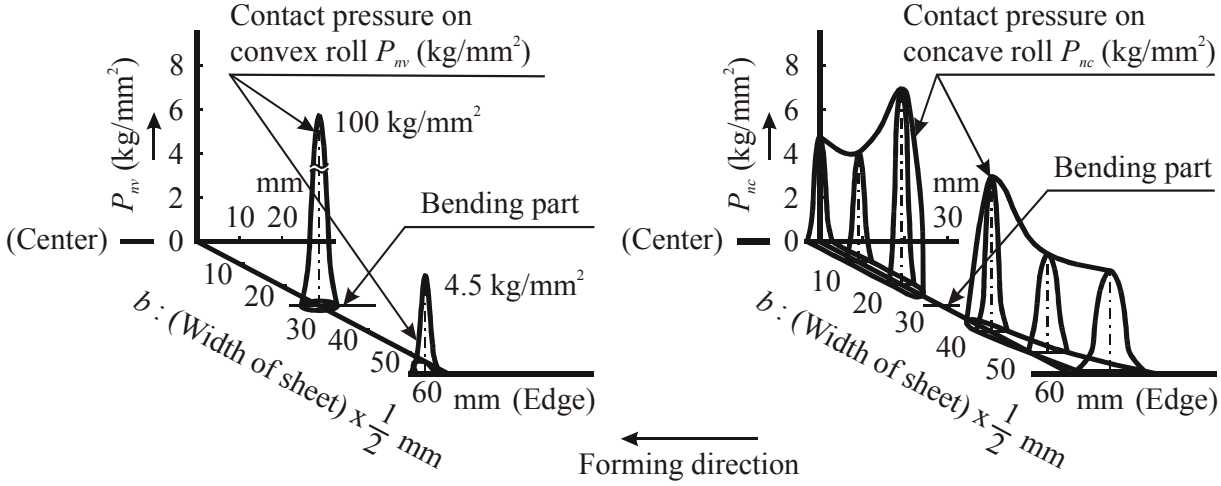

Fig. 31. Few typical examples of roll-strip contact pressure distribution during CRF trapezoidal profile [85].

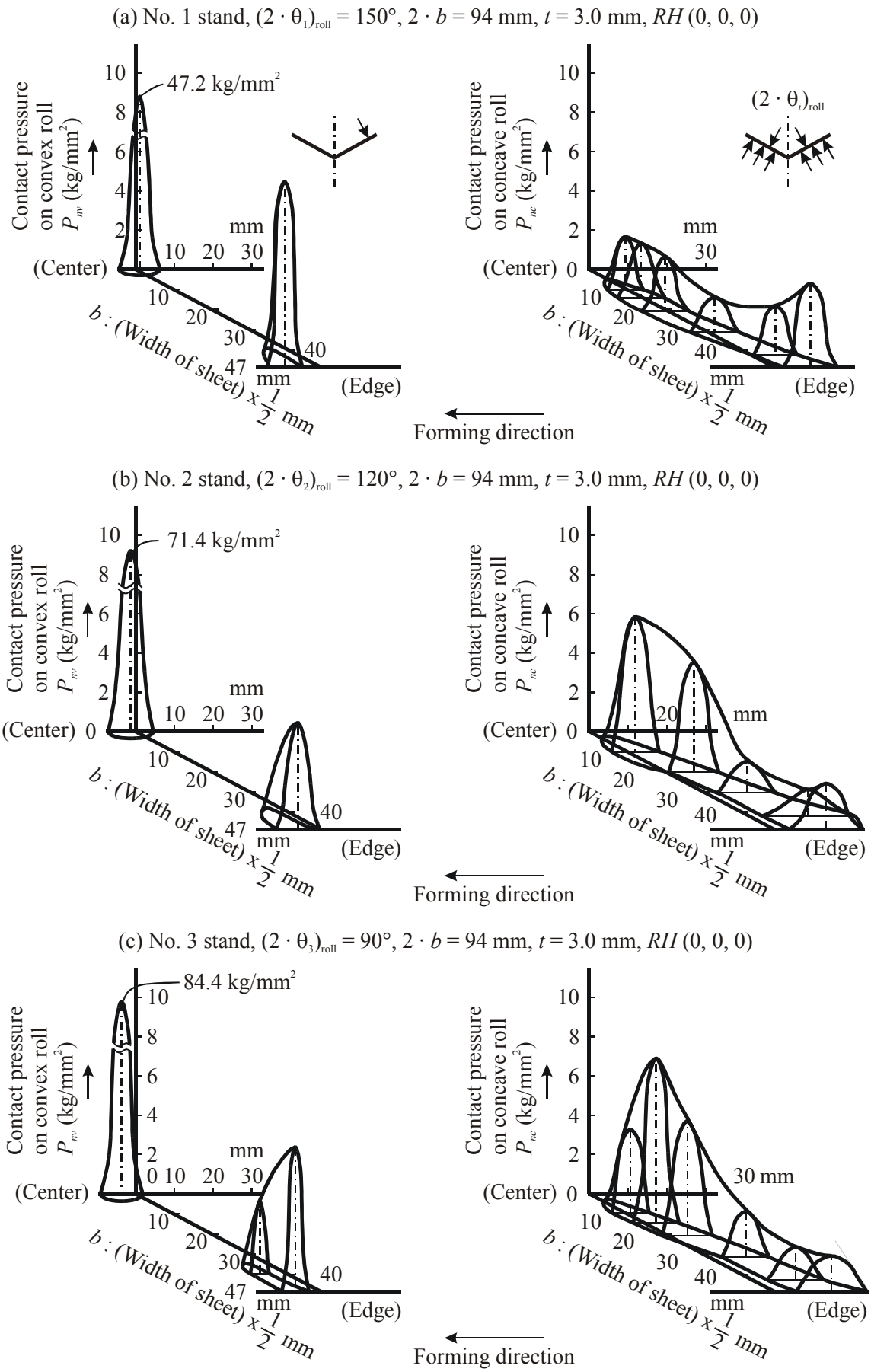

Fig. 32. Few typical examples of roll-strip contact pressure distribution during CRF V-type profile [85].

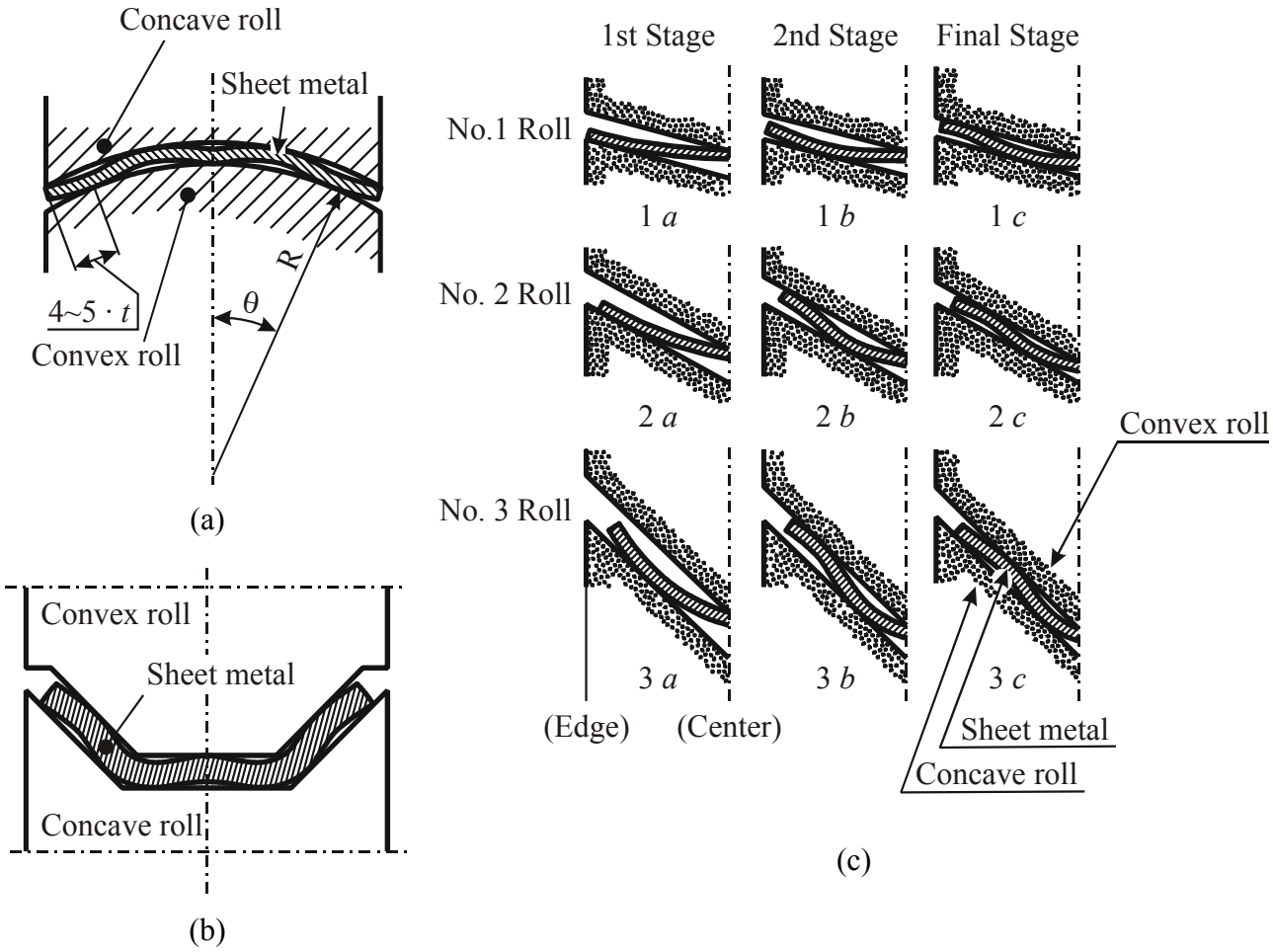

Fig. 33. Examples of strip deformation behaviour in the narrowest position of circular roll gap (a), of trapezoidal roll gap (b) and at inletting steps into roll gap for V-type profile (c) [85].

Suzuki et al [85] proposed no method of computation for contact pressure distribution in considered conventional types of the CRF processes, that degrade the value of their experimental results for the CRF process design. Although Suzuki's et al [85] approach was followed by Kiuchi [44], the results obtained by this method are only qualitative and also cannot be extrapolated to the more energy efficient vertical the CRF process proposed by Nakajima et al [63] for the circular ERW pipe. The new vertical the CRF process has the reduced roll-strip contact area with a contact pressure distribution totally different from that of the conventional circular ERW pipe the CRF process.

Later research of the conventional circular ERW pipe the CRF process by Walker and Pick [98] revealed that the strip is not in full contact with the forming rolls of the real industrial CRF mill, so that the actual profile shape is substantially different than the theoretical shape predicted from the roll-stand geometry. This inevitably affects the roll-strip contact pressure distribution.

An optimal shape design of contact surfaces can itself help to reduce tools wear and power losses. The approaches to optimal shape of arbitrary contact surfaces design were reviewed by Páczelt and Mróz [73].

The roll-strip contact pressure distribution still remains unstudied for CRF. The experimental investigation of contact pressure distribution is difficult and very expensive. Its theoretical study has to be sensitive to complex roll-strip contact geometry. The use of exact strip geometry modelling [8, 33] for contact stress analysis seems to be more promising compared to use of geometry approximations [97, 98].

3.3.2. Lubrication

The decision to use a lubricant is motivated by the aims of reducing sectional distortion due to heat; obtaining better surface finish by reducing scuffing and by "flushing" away debris from between the rolls; reducing wear and prolonging tool life [9, 26, 74].

The influence of lubricant on forming load was neglected and even denied in the early stages of CRF technology development. But, Starchenko and Chelovan's research showed that the effect of lubrication must be taken into account [81]. They performed experiments with two lubricants: grade 20 industrial oil and castor oil. Their experiments demonstrated that the industrial oil reduces the forming load by 8 ÷ 12 %, but castor oil reduces this load by 10 ÷ 15 % (fig. 34). Moreover, the effect of lubrication becomes more evident as the thickness or the width of the strip increase [81].

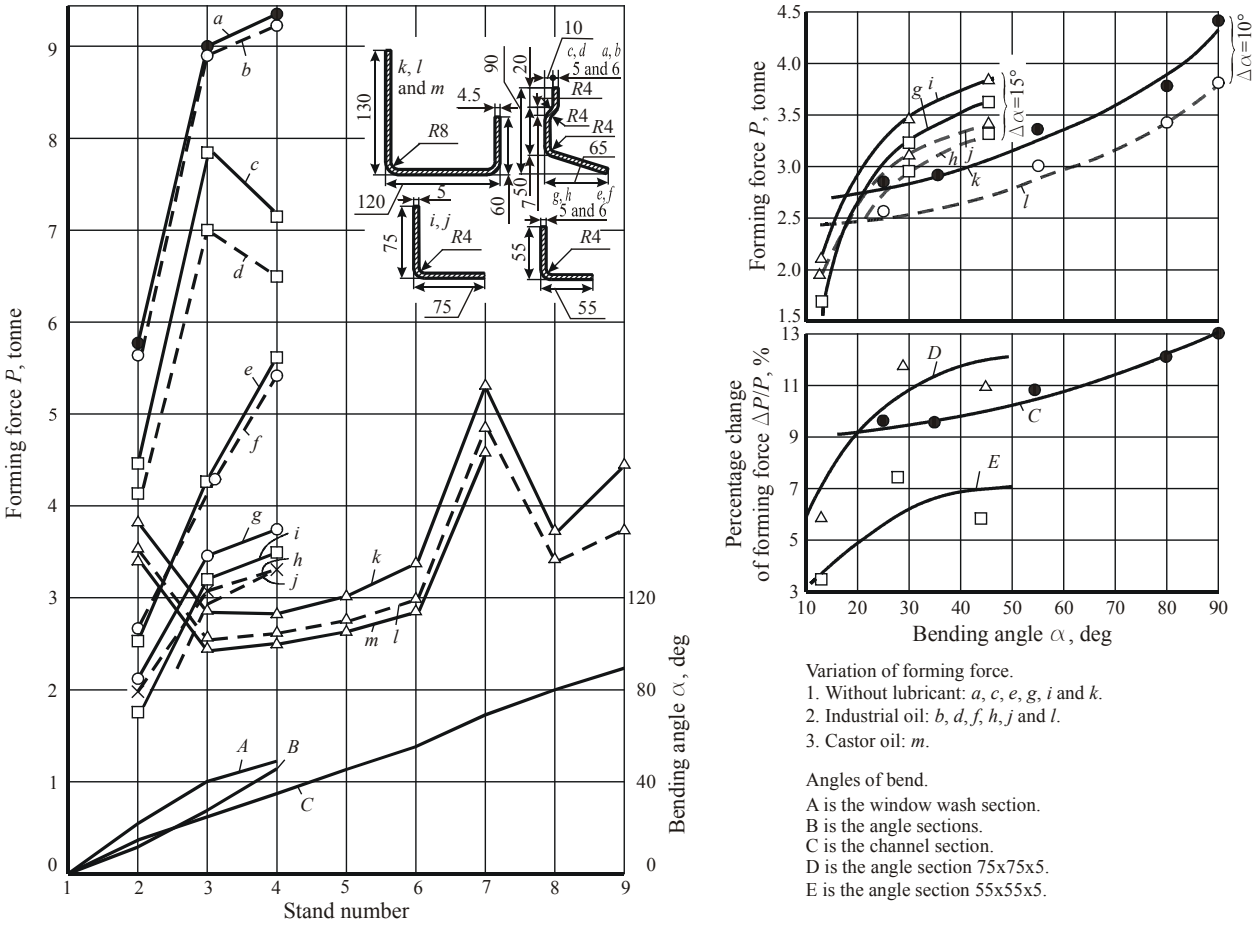

Fig. 34. Effect of lubrication on the CRF process [81].

However, although lubrication has several advantages, unnecessary or incorrect application of a lubricant can similarly result in many significant disadvantages. These include sectional distortion, due to differential friction and cooling, surface defects, staining, blushing, blistering and peeling and the need for auxiliary degreasing operations [9]. As such, many products are roll formed without lubricant [9]. A good investigation and analysis of the most common lubricant problems is provided by Ivaska [36].

3.3.3. Friction and wear of contact surfaces

The friction in roll-strip contact has a 3D nature and embodies both rolling and sliding friction components. Furthermore, the assumption that friction forces are parallel to the motion direction is satisfied for arbitrary surfaces only approximately [24]. Modern computational methods for friction modelling were reviewed by Laursen [49]. However the existing models

of the CRF process analysis usually neglect the friction effect or incorporate it using the simplest Coulomb's law formulation [5, 15, 80].

Contact friction has two components resulting in power dissipation:

1) adhesive friction related to the power expended on making and breaking adhesion bonds formed in the points of contact of sliding surfaces;
2) mechanical friction related to the power expended on cyclic deformation of the contacting bodies.

The adhesive friction depends on the properties of the contacting bodies and on the friction conditions.

The mechanical friction depends on the mechanical properties of the bodies, the contact geometry, the applied forces etc., and can be studied by the method of contact mechanics.

The adhesive and mechanical components of friction are usually considered as independent in tribology, although some experiments controvert this statement [60].

Godet [23] proposed a general approach to modelling the adhesive interaction in sliding contact in the presence of a thin layer between the contacting bodies, however no mathematical modelling was provided.

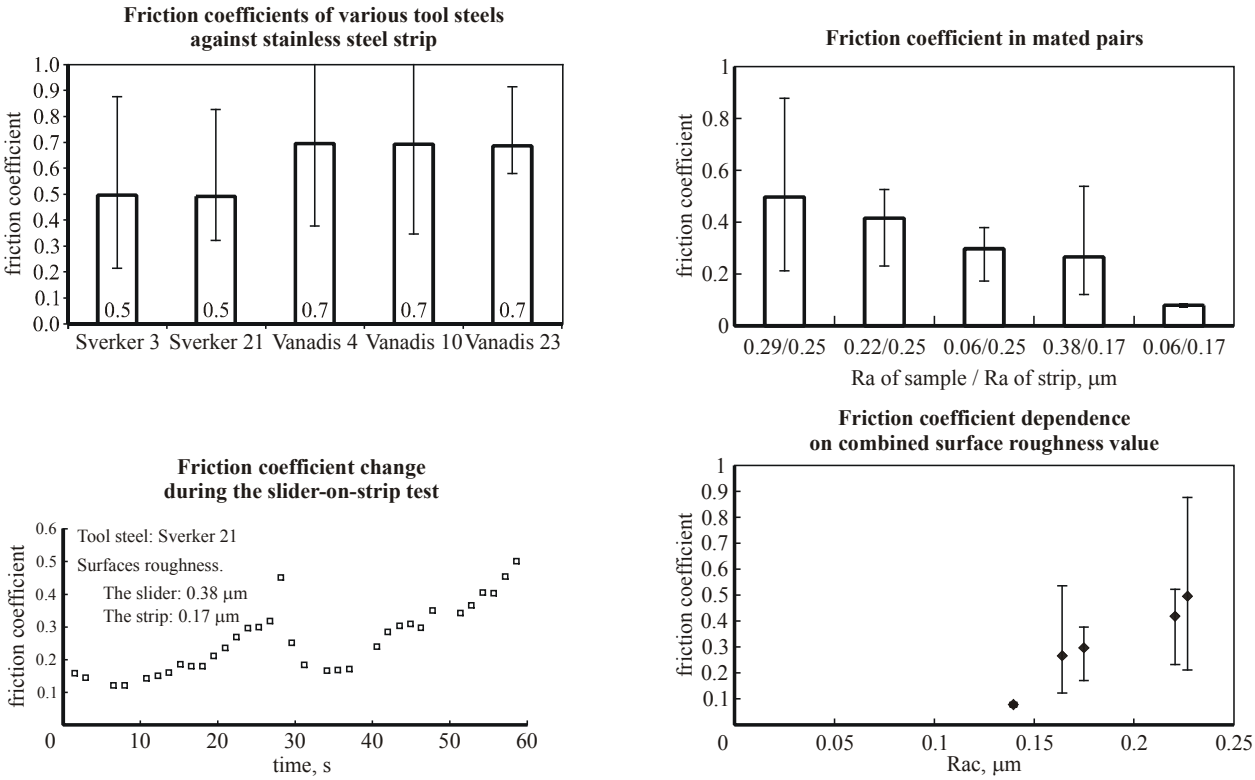

Fig. 35. Friction in contact with a strip [53]

Määttä et al [53] studied the friction and adhesion of stainless steel strip against tool steels. They considered an unlubricated process and assumed that the friction obeys Coulomb's law. The friction coefficients varied within wide limits during the experiment and were very different for different tool steels (see fig. 35) [53]. Määttä et al [53] proposed to analyse the effect of surface roughness using a combined Ra value denoted as Ra_C:

$$\frac{1}{Ra_C^2} = \frac{1}{Ra_1} + \frac{1}{Ra_2^2}, \tag{2}$$

where Ra_1 and Ra_2 are the surface roughness of the slider and the strip respectively.

The expression (2) shows that the surface roughness of the strip has a greater effect [53].

Määttä et al showed that the friction of stainless steel strip against the slider of tool steel was mainly caused by adhesion between the two materials and the adhesion increases when the oxide layers on the metal surfaces are broken. The tool steel did not wear during the tests.

The wear occurred in the stainless steel, which accumulated on the surface of the tool steel. The mechanical component of friction included an abrasive part caused by the stainless steel wear debris on the tool steel surface.

Konyukhov et al [48] proposed an orthotropic adhesion-orthotropic friction model that allows qualitative description of stick-slip phenomena.

The analysis of the contact problem solutions, taking into account inelastic properties of solids and friction, allows the establishment of the dependence of contact characteristics on the mechanical properties of bodies and the contact conditions [24].

Hashimoto et al proposed a non-linear sliding friction law taking into account the frictional work quantity and normal pressure [27]. The history independence of fiction coefficient makes this law more advantageous than typical Amontons-Coulomb's laws.

Adhesive and mechanical friction components take place both in sliding and in rolling contact. The qualities of roll-strip contact have to be determined to analyse the friction and wear in it.

Ling [51] reviewed applications of fractals to tribology.

Fractal descriptions of engineering surfaces have been proposed by Majumdar et al [54, 55, 56], Stupak et al [83], Vandenberg and Osborne [91], Wehbi et al [102], Yordanov and Ivanova [107], Brown et al [12]. Several approaches for describing contact faces with fractals were reviewed by Mainsah et al [3]. Fractal theories of contact mechanics have been developed by Wang and Komvopoulos [99], Warren and Krajcinovic [100], Tudor et al [89]. However some of the above works devoted to fractals should be treated with caution, as not all authors have distinguished between self-similar and self-affine fractals [3] and different methods of calculation can yield significantly different numerical values of the fractal parameters [76]. Although the research area of fractal geometry is well developed [51, 82], no attempts at its application to the CRF process analysis have been published.

4. Conclusion

Both the quality of CRF products and the service life of forming rolls are strongly affected by contact and dynamic phenomena appearing during the CRF process. But the contact and dynamic phenomena remain unstudied as a modelling problem in CRF. The literature review has revealed the shortage of empirical and theoretical results relevant to contact pressure distribution and wear prediction in CRF. This was caused by difficulties in carrying out the experimental research of roll-strip contact.

The last 30 years were characterized by rapid development of computer technology. It opens wide prospects for numerical analysis of the CRF process and for determination of optimum conditions for CRF, taking into consideration tool wear and friction in roll-strip contact. Such analysis of the tool wear and friction requires accurate solution of the roll-strip contact mechanics that takes into account the latest experimental results on friction and wear of contact surfaces and is combined with the algorithms of contact area determination.

The empirical results concerning roll-strip contact pressure distribution are contradictive. Sliding in roll-strip contact is not studied properly in CRF. No results were found concerning roll-strip sliding in CRF. Consequently, there is an absence of published results on prediction of tool wear in CRF.

5. References

1. *Designer's Guide to Roll Forming.* Precision Metal, 1976. **34**(4): p. 44-46.
2. *Contour Roll Forming*, in *ASM Handbook Vol. 14: Forming and Forging*. 1988, ASM International.
3. *Metrology and Properties of Engineering Surfaces*, ed. E. Mainsah, Greenwood, J.A., Chetwynd, D.G. 2001, Boston, Dordrecht, London: Kluwer Academic Publishers.
4. *Automotive Steel Design Manual*. 6.1. Revised ed. 2002: American Iron & Steel Institute.
5. Alsamhan, A., P. Hartley, and I. Pillinger, *The computer simulation of cold-roll-forming using FE methods and applied real time re-meshing techniques.* Journal of Materials Processing Technology, 2003. **142**(1): p. 102-111.
6. Angel, R.T., *Designing Tools for Cold Roll Forming.* The Iron Age, 1949. **164**(18): p. 83-88.
7. Baba, Z., *Studies on Roll Forming of Electric Resistance Welded Thin Walled Steel Tube.* Sumitomo Metals, 1963. **15**(2): p. 19-28.
8. Bazilevs, Y., et al., *Isogeometric Analysis: Approximation, stability and error estimates for h-refined meshes*. 2006, The Institute for Computational Engineering and Sciences: Austin. p. 58.
9. Bhattacharyya, D., *Composite Sheet Forming*. Composite Materials Series, ed. D. Bhattacharyya. Vol. 11. 1997: Elsevier.
10. Boyens, D.T., *Cold roll forming of trapezoidal and rectangular channel sections and the effect of residual strain on the longitudinal curvature for different materials*, in *Mechanical Engineering Project Report ME 07*. 1985, The University of Auckland: Auckland.
11. Brown, B.W., *The effect of various material properties on the residual membrane stresses generated in cold roll forming trapezoidal and rectangular channel sections*, in *Mechanical Engineering Project Report ME 03*. 1984, The University of Auckland: Auckland. p. 145.
12. Brown, C., W. Johnsen, and K. Hult. *Scale-sensitivity, fractal analysis and simulations*. in *7th International Conference on Metrology & Properties of Engineering Surfaces*. 1997. Göteborg.
13. Brunet, M., B. Lay, and P. Pol, *Computer aided design of roll-forming of channel sections.* Journal of Materials Processing Technology, 1996. **60**(1-4): p. 209-214.
14. Brunet, M., S. Mguil, and P. Pol, *Modelling of a roll-forming process with a combined 2D and 3D FEM code.* Journal of Materials Processing Technology, 1998. **80-81**: p. 209-214.
15. Brunet, M. and S. Ronel-Idrissi, *Finite element analysis of roll-forming of thin sheet metal.* Journal of Materials Processing Technology, 1994. **45**(1-4): p. 255-260.
16. Carson, W.J., *The effect of residual strain on longitudinal curvature induced when cold roll forming trapezoidal or channel sections of different materials*, in *Mechanical Engineering Project Report ME 09*. 1985, The University of Auckland: Auckland.
17. Cherevik, Y.I. and V.T. Vyshinskii. *The approaches to improving the dynamic characteristics of the piping cold roll forming mills main drives*. in *Scientific and technical conference on "Problems of Mechanization of Mining and Metallurgical Complexes 2002"*. 2002. Dnepropetrovsk, Ukraine: National Mining University of Ukraine. In Rusian.
18. Chiang, K.F., *A Study of Cold Roll Forming*, in *Mechanical Engineering Project Report ME 06*. 1982, The University of Auckland: Auckland. p. 58.
19. Davydov, V.I. and M.P. Maksakov, *Manufacture of Angular Section on Roll Forming Machines*. Extended and revised edition ed. 1959, Moscow: Metallurgizdat. In Russian.
20. Ding, S.C., *A Theoretical and Experimental Study of the Roll Forming Process*, in *The Department of Mechanical Engineering*. 1998, The University of Auckland: Auckland.
21. Ding, S.C. and J.L. Duncan, *Instability in bending-under-tension of aged steel sheet.* International Journal of Mechanical Sciences, 2004. **46**: p. 1471-1480.
22. Farzin, M., M. Salmani Tehrani, and E. Shameli, *Determination of buckling limit of strain in cold roll forming by the finite element analysis.* Journal of Materials Processing Technology, 2002. **125-126**: p. 626-632.
23. Godet, M., *The third-body approach: a mechanical view of wear.* Wear, 1984. **100**(1-3): p. 437-452.
24. Goriacheva, I.G., *Contact mechanics in tribology*. 1998, Boston: Kluwer Academic Publishers.

25. Greenwood, J., *The Third Industrial Revolution: Technology, Productivity, and Income Inequality*. 1997, Washington: American Enterprise Institute for Public Policy Research.
26. Halmos, G.T., *Roll Forming Handbook*, ed. G.T. Halmos. 2006: CRC Press.
27. Hashimoto, K., et al., *Proposal of Nonlinear Friction Law Taking Account of Frictional Work Quantity and Normal Pressure as State Variables: Assessment of Sheet Formability by Nonlinear Friction Model II.* Journal of the Japan Society for Technology of Plasticity, 2006. **47**(544).
28. Hayashi, Y. and M. Takatani. in *31st Japanese Joint Conference for the Technology of Plasticity*. 1980. Tokyo.
29. Hayes, N., *The Occurrence of Edge Wave in Cold Roll Forming*, in *PME Report 92/23*. 1992, The University of Auckland: Auckland.
30. Hicks, T., *The Occurrence of Edge Wave in Cold Roll Forming Channel*, in *PME Report 92/24*. 1992, The University of Auckland: Auckland.
31. Hira, T., et al., *Effect of mechanical properties of steel sheets on web buckling behaviour in cold roll forming of siding board.* Journal of the Japan Society for Technology of Plasticity, 1979. **20**: p. 933-939.
32. Hobbs, R.M. and J.L. Duncan, *Roll Forming*. 1979, Ohio: Metals Engineering Institute, American Society of Metals.
33. Hughes, T.J.R., J.A. Cottrell, and Y. Bazilevs, *Isogeometric analysis: CAD, finite elements, NURBS, exact geometry and mesh refinement.* Computer Methods in Applied Mechanics and Engineering, 2005. **194**(39-41): p. 4135-4195.
34. Ingvarsson, L., *Cold-forming Residual Stresses: Effect on Buckling*, in *The Third International Specialty Conference on Cold-formed Steel Structures*. 1975: St. Louis, USA.
35. Ingvarsson, L. *Cold Forming Residual Stresses in Thin-walled Structures*, in *International Conference on Thin Walled Structures*. 1979. Glasgow, UK: Halsted press.
36. Ivaska, J., *Analysis of Lubrication Problems in Roll Forming*, in *High production roll forming*. 1984, Society of manufacturing engineers: Michigan. p. 110-122.
37. Jimma, T. and H. Ona. *Optimum Roll Pass Schedules on the Cold Roll Forming Process of Symmetrical Channels*. in *21st International Machine Tool Design and Research Conference*. 1980.
38. Kato, K., *A Basic Study on Cold Forming Technique*, in *Tech Re Overseas*. 1963, Nippon Kokan Kubushiki Kaisha. p. 44-54.
39. Kato, K., Y. Saito, and H. Shinto, *Effect of Metal Properties on Shape of Roll Formed Product — Circular Arc Section.* Technology Reports of the Osaka University, 1980. **30**(1551/1582): p. 405-410.
40. Kimura, H., *Edge Waves of Thin Wall Roll Formed Product: Fundamental Study on Roll Forming Process.* Sumitomo light metal technical reports, 1974. **15**(4): p. 252-257.
41. Kirkland, W.G., *Cold Forming Practice in the United States.* Iron and Steel Engineer, 1959. **36**(11): p. 134-149.
42. Kiuchi, M., *Analytical Study on Cold-Roll-Forming Process — Stress Distribution in Sheet Metal Subjected to Various Forms of Deformation at Forming Process and Effects of Strain-Path and Behavior of Redundant Strain Components on Product Shape*, in *Report of the Institute of Industrial Science*. 1973, University of Tokyo: Tokyo. p. 43.
43. Kiuchi, M. *Distribution of Contact Pressure Measured by Wire Mesh Method in Roll-forming Process through Tandem Mills*. in *1st International Conference on rotary metalworking processes*. 1979. London.
44. Kiuchi, M., *Recent Development of Roll-Forming in Japan.* International Journal of Machine Tools & Manufacture, 1989. **29**(1): p. 63-77.
45. Kiuchi, M., K. Shintani, and M. Tozawa, Journal of the Japan Society for Technology of Plasticity, 1980. **21**: p. 339-346. In Japanese.
46. Kiuchi, M., K. Shintani, and M. Tozawa, Journal of the Japan Society for Technology of Plasticity, 1980. **21**: p. 405-412. In Japanese.

47. Kokado, J.I. and Y. Onoda, *On Longitudinal Curvature and Transitions of Strain of Sheet Steel in Forming a Groove with Wide Flanges by Cold Roll Forming.* Kyoto University, Faculty of Engineering Memoirs, 1974. **36**(4): p. 443-457.
48. Konyukhov, A., K. Schweizerhoft, and P. Vielsack. *On models of contact surfaces including anisotropy for friction and adhesion and their experimental validations*, in *III European Conference on Computational Mechanics: Solids, Structures and Coupled Problems in Engineering*. 2006. Lisbon, Portugal: Springer.
49. Laursen, T.A., *Computational Contact and Impact Mechanics*. 2002, Berlin, Heidelberg: Springer-Verlag.
50. Lejchenko, M.A., *Manufacture of Bent Sections with Roll Forming Machines.* Stal', 1955. **25**(6): p. 526-534. In Russian.
51. Ling, F.F., *Fractals, engineering surfaces and tribology.* Wear, 1990. **136**(1): p. 141-156.
52. Looi, B.C., *A study of cold roll forming*, in *Mechanical Engineering Project Report ME 32*. 1983, The University of Auckland: Auckland.
53. Määttä, A., P. Vuoristo, and T. Mäntylä, *Friction and adhesion of stainless steel strip against tool steels in unlubricated sliding with high contact load.* Tribology International, 2001. **34**: p. 779-786.
54. Majumdar, A. and B. Bhushan, *Role of Fractal Geometry in Roughness Characterization and Contact Mechanics of Surfaces Surfaces.* Journal of Tribology, 1990. **112**: p. 205 - 216.
55. Majumdar, A. and B. Bhushan, *Fractal Model of Elastic-Plastic Contact Between Rough Surfaces.* Journal of Tribology, 1991. **113**(1): p. 1 - 11.
56. Majumdar, A. and C.L. Tien, *Fractal characterization and simulation of rough surfaces.* Wear, 1990. **136**(2): p. 313-327.
57. Masuda, M., et al., *Fundamental Research on the Cold Roll Forming of Metal Strips.* Bulletin of JSME, 1964. **7**(28): p. 827-834.
58. Mednikov, Y.A., *Length of the Uniform Transition Zone and Relative Expansion of the Edges of Strip when Forming into Tube.* Stal', 1963. **33**(4): p. 301-303. In Russian.
59. Miyamoto, Y. and S. Hawa, *Effect of Tensile Flow Properties of Titanium Sheets on Web-Buckling Behaviour in Cold Roll-forming of Wide Profile.* ISIJ International, 1991. **31**(8): p. 863-869.
60. Moore, D.F., *Principles and Applications of Tribology*. Materials Science and Technology, ed. D.W. Hopkins. 1975, Oxford: Pergamon Press. 388.
61. Mynors, D.J., et al. *Controlling the Cold Roll Forming Design Process*, in *CIRP 2006 General Assembly: Session on Forming (F)*. 2006. Paris: CIRP.
62. Naidenov, A.A. and V.B. Kaluzhskii, *Roll Pass Design for Multiple Stand Piecework Cold Forming Mills.* Stal', 1963. **33**(1): p. 57-61. In Russian.
63. Nakajima, K., et al., *Development of New Vertical Roll Forming Process for Electric Resistance Welded Pipe*, in *Nippon Steel Technical Report*. 1980, Nippon Steel. p. 127-144.
64. Nakako, T., T. Nakahara, and H. Asada. *Mechanism of Occurrence of Pocket Wave and Effect of Mechanical Properties of Steel Sheets on Pocket Wave in Cold-Roll-Forming of Wide Profiles*. in *The 50th Japanese Joint Conference for the Technology of Plasticity*. 1999. Fukuoka.
65. Okamura, Y. and K. Takada, Journal of the Japan Society for Technology of Plasticity, 1979. **20**(216): p. 889-896.
66. Ona, H. and T. Jimma. *Prevention of Oil Canning and Edge Buckling in the Cold Roll Forming Process of Wide Profiles*, in *2nd International Conference on rotary metalworking processes*. 1982.
67. Ona, H. and T. Jimma, *On Method of Roll Design for Cold Roll Forming of Light Gauge Steel Members — Research on the High Accuracy Cold Roll Forming Process of Channel Type Cross Section VII.* Journal of the Japan Society for Technology of Plasticity, 1983. **24**(270): p. 707-714.
68. Ona, H. and T. Jimma, *Prevention of Shape Defects in the Cold Roll Forming Process of Wide Profiles.* Bulletin of Research Laboratory of Precision Machinery and Electronics, 1984. **53**: p. 1-13.

69. Ona, H., T. Jimma, and N. Fukaya, *Experiments into the Cold Roll-Forming of Straight Asymmetrical Channels.* Journal of Mechanical Working Technology, 1983. **8**(4): p. 273-291.
70. Ona, H., T. Jimma, and M. Shimada, *Experiment on the Edge Buckling, Crack and Distortion of Wide Profiles — Research on the High Accuracy Cold Roll Forming Process of Channel Type Cross Section V*. Journal of the Japan Society for Technology of Plasticity, 1982. **23**(259): p. 809-815.
71. Ona, H., et al., *Experiment on the Pocket Wave of Wide Profiles — Research on the High Accuracy Cold Roll Forming Process of Channel Type Cross Section IV*. Journal of the Japan Society for Technology of Plasticity, 1982. **23**(258): p. 664-671.
72. Ona, H., H. Watari, and T. Nakako, *Production method on pipe of thin-spring steel sheet.* Journal of Materials Processing Technology, 2001. **115**(1): p. 92-96.
73. Páczelt, I. and Z. Mróz. *Contact optimization problems associated with the wear process*, in *XXI International Congress of Theoretical and Applied Mechanics (ICTAM 2004)*. 2004. Warsaw, Poland: Springer Verlag.
74. Panton, S.M., *Computer aided form roll design*. 1987, The University of Aston in Birmingham: Birmingham. p. 321.
75. Rhodes, A., A.S. Boardman, and D.H. McIntosh. *Computer Aided Design and Manufacture of Rolls for Cold Roll Forming Machines*. in *1st International Conference on rotary metalworking processes*. 1979. London.
76. Russ, J.C., *Fractal Surfaces*. 1994, New York: Plenum Press.
77. Russell, J.D. and N.L. Kuhn, *A Mathematical Model of Sheet Bending Applied to Corrugating.* Journal of the Australian Institute of Metals, 1966. **11**(1): p. 38-46.
78. Sachs, G., *Sheetmetal Fabricating*. 1966: Reinhold Publishing Corporation.
79. Schulze, G., *Data for the Development and Application of Forming Machines.* Maschinenbautechnik, 1959. **8**(4): p. 181-191.
80. Sheu, J.-J. *Simulation and optimization of the cold roll-forming process*, in *Numerical Methods in Industrial Forming Processes (NUMIFORM 2004)*. 2004. Columbus, USA.
81. Starchenko, D.I. and M.I. Chelovan, *Effects of lubricants on roll forming force.* Stal', 1968. **38**(2): p. 139-140.
82. Stoyan, D. and H. Stoyan, *Fractals, Random Shapes and Point Fields: Methods of Geometrical Statistics*. Wiley series in probability and mathematical statistics. 1994, Brisbane: John Wiley & Sons.
83. Stupak, P.R., C.Y. Syu, and J.A. Donovan, *The effect of filtering profilometer data on fractal parameters.* Wear, 1992. **154**: p. 109-114.
84. Suzuki, H., M. Kiuchi, and S. Nakajima, *Experimental Investigation on Cold-Roll-Forming Process: effects of forming factors and process variables on product shape, forming loads and torques in forming process for fundamental cross-sectional profiles*. 1972, The Institute of Industrial Science, the University of Tokyo: Tokyo. p. 1-89.
85. Suzuki, H., et al., *Experimental Investigation on Cold-Roll-Forming Process II: distribution of contact pressure on interface between sheet metal and forming rolls in roll-forming process through tandem mills*. 1976, The Institute of Industrial Science, the University of Tokyo: Tokyo. p. 56.
86. Suzuki, H., et al., *Investigation into Deformation Behaviours of Sheets in Cold Roll Forming Process of Wide Profile with Trapezoidal Grooves — Experimental Study on Cold Roll Forming of Wide Profiles V*. Journal of the Japan Society for Technology of Plasticity, 1977. **18**(196): p. 365-372.
87. Tomita, Y. and H. Shao. *Buckling Behavior in Thin Sheet Metal Subjected to Nonuniform Membrane-Type Deformation*. in *The Asia-Pacific Symposium on Advances in Engineering Plasticity and Its Applications (AEPA'92)*. 1992. Hong Kong: Elsevier.
88. Toyooka, T., *Computer simulation for tube-making by the cold roll-forming process*, in *Department of Mechanical and Electrical Engineering*. 1999, The University of Aston in Birmingham: Birmingham. p. 321.

89. Tudor, A., T. Savu, and D. Pavelescu. *The bearing capacity of fractal engineering surfaces*, in *7th International Conference on Metrology & Properties of Engineering Surfaces*. 1997. Göteborg.
90. van den Boogaard, A.H., H.H. Wisselink, and J. Huétink, *Do Advanced Material Models Contribute to Accuracy in Industrial Sheet Forming Simulations?* Advanced Materials Research, 2005. **6-8**: p. 71-80.
91. Vandenberg, S. and C.F. Osborne, *Digital image processing techniques, fractal dimensionality and scale-space applied to surface roughness.* Wear, 1992. **159**: p. 17-30.
92. Vanderploeg, E.J., *Designing Rolls for Cold Roll Forming.* Machinery, 1948. **54**: p. 176-180.
93. Vanderploeg, E.J., *Tooling for Cold Roll Forming and Auxiliary Operations.* Machinery, 1948. **54**: p. 172-176.
94. Vanderploeg, E.J., *Forming Metal Shapes by Cold Rolling.* Machinery, 1948. **54**: p. 153-158.
95. Vanderploeg, E.J., *Roll Forming — Simple Method for Designing Rolls.* Tool Engineer, 1953(October): p. 59-65.
96. Vanderploeg, E.J., *Getting Most Out of Roll Formed Design.* Product Engineering, 1962. **33**(24): p. 75-78.
97. Walker, T.R. and R.J. Pick, *Approximation of the axial strains developed during the roll forming of ERW pipe.* Journal of Materials Processing Technology, 1990. **22**(1): p. 29 - 44.
98. Walker, T.R. and R.J. Pick, *Developments in the geometric modelling of an ERW pipe skelp.* Journal of Materials Processing Technology, 1991. **25**: p. 35-54.
99. Wang, S. and K. Komvopoulos, *A fractal theory of the temperature distribution at elastic contacts of fast sliding surfaces.* Journal of Tribology, 1995. **117**: p. 203-215.
100. Warren, T.L. and D. Krajcinovic, *Fractal models of elastic-perfectly plastic contact of rough surfaces based on the Cantor set.* International Journal of Solids and Structures, 1995. **32**(19): p. 2907-2922.
101. Watari, H. and H. Ona, *Characteristic features of shape defects occurring in the cold roll forming of pre-notched products.* Journal of Materials Processing Technology, 1998. **80-81**: p. 225-231.
102. Wehbi, D., C. Roques-Carmes, and C. Tricot, *The perturbation dimension for describing rough surfaces.* International Journal of Machine Tools & Manufacture, 1992. **32**(1-2): p. 211-216.
103. Weimar, G., *The State of Development of Cold Roll Forming: a Review of Published Work.* Bänder, Bleche, Rohre, 1967. **8**: p. 308-324.
104. Wen, B. and R.J. Pick, *Modelling of skelp edge instabilities in the roll forming of ERW pipe.* Journal of Materials Processing Technology, 1994. **41**(4): p. 425-446.
105. Yamakawa, T., *Deformation of Strip during Single-stage V-shape Roll Forming*, in *Sosei to Kato, No. 35*. 1963. p. 783-795.
106. Yoder, C.M., *Cold Roll Forming and Bending.* Iron and Steel Engineer, 1937. **14**(2): p. 13-18.
107. Yordanov, O.I. and K. Ivanova, *Description of surface roughness as an approximate self-affine random structure.* Surface Science, 1995. **331-333**: p. 1043-1049.
108. Zuev, L.B., et al., *A new type of plastic deformation waves in solids.* Applied Physics A: Materials Science & Processing, 2000. **71**(1): p. 91-94.